DON AU

Reprinted from

CATENA

Catena 32 (1998) 245–280

From Oxisols to Spodosols and Histosols: evolution of the soil mantles in the Rio Negro basin (Amazonia)

Didier Dubroeucq *, Boris Volkoff

ORSTOM, 32 avenue H. Varagnat, 93143 Bondy Cedex, France

ELSEVIER

CATENA

Scope of the journal

Catena publishes papers describing original field and laboratory investigations and reviews on geo-ecology and landscape evolution with emphasis on interdisciplinary aspects of soil, hydrology and geomorphology. It aims to disseminate new knowledge and foster better understanding of the physical environment, of evolutionary sequences that have resulted in past and current landscapes, and of the natural processes that are likely to determine the fate of our terrestrial environment.

Papers within any one of the above topics are welcome provided they are of sufficiently wide interest and relevance.

Publication information

Catena (ISSN 0341-8162). For 1998 volumes 32–34 are scheduled for publication. Subscription prices are available upon request from the publisher. Subscriptions are accepted on a prepaid basis only and are entered on a calendar year basis. Issues are sent by surface mail except to the following countries where air delivery via SAL is ensured: Argentina, Australia, Brazil, Canada, Hong Kong, India, Israel, Japan, Malaysia, Mexico, New Zealand, Pakistan, PR China, Singapore, South Africa, South Korea, Taiwan, Thailand, USA. For all other countries airmail rates are available upon request. Claims for missing issues must be made within six months of our publication (mailing) date.

(see further inside back cover)

ELSEVIER

Catena 32 (1998) 245–280

CATENA

From Oxisols to Spodosols and Histosols: evolution of the soil mantles in the Rio Negro basin (Amazonia)

Didier Dubroeucq *, Boris Volkoff

ORSTOM, 32 avenue H. Varagnat, 93143 Bondy Cedex, France

Received 28 October 1993; accepted 29 January 1998

Abstract

The Upper Rio Negro basin, under a constantly humid equatorial climate, is a low-altitude peneplain of more than 165,000 km^2. Prevailing soils are Oxisols and Spodosols, and their distribution is usually related to the lithology of the parent materials; Spodosols being generally associated with sandy deposits. After exploratory surveys in this extensive region, six major soil-geomorphic units have been identified in which selected toposequences have been studied by means of micromorphological, chemical and mineralogical analyses. Detailed field analysis of the horizonation of the soil mantle has been carried out in three sequences consisting of Oxisols, Ultisols and Spodosols. Results show that sharp transitions, within distances of less than one hundred meters, separate the Oxisols from the Spodosols. However, the arrangement of the horizons in the soil mantle and similarities in micromorphological features, chemical composition and mineral components between the adjacent horizons are evidences that genetic relationships link contiguous profiles. The authors propose an alternative explanation for this soil distribution, based on the lateral transformation of Oxisols and Ultisols into Spodosols, and on the lateral evolution of the giant Spodosols into Histosols (peat) and waterlogged Ultisols. Interpretative models of landscape evolution as consequence of soil evolution are thus proposed.

Keywords: Pedogenesis; Oxisol; Spodosol; Histosol; Landform evolution; Amazon basin

* Corresponding author.

0341-8162/98/$19.00
PII S0341-8162(98)00045-9

1. Introduction

The high mountain ranges and typical tablelands ('tepuis'), which rise up to 2500 m in southern Venezuela and Guyana, decrease towards the edges of the Guyana Shield and disappear entirely at the West of the Middle Orinoco and Casiquiare rivers. There, lowlands extend widely throughout Colombia and Brazil, forming a large apparently flat basin which extends over 165,000 km^2, the overall altitude of which is between 200 and 70 m.

A deep lateritic weathering profile with a continuous Oxisol mantle characterizes the upper levels of the Guyana Shield (Aleva, 1981; Dubroeucq et al., 1988). In contrast, the lower plains as observed and emphasized by the first Amazonian soil surveyors (Klinge, 1965; Sombroek, 1966) display very different soils: Oxisols, Ultisols, Spodosols and Histosols (Soil Survey Staff, 1975, 1990). The presence of such a diversity of soil types raises questions concerning their origin.

In the Amazon region, lithology has been considered as the main factor of soil distribution. Quaternary sandy alluvial sediments in contact with the rock basement or with lacustrine clayey deposits (Belterra formation), were supposed to explain the Spodosol–Oxisol distribution (Klinge, 1965; Putzer, 1984). Following the same reasoning, Spodosols in the Rio Negro and middle Rio Branco plains were believed to be the result of a large-scale denudational event: after the capture of some of the Orinoco and Esequibo tributaries by the Amazon, early Pleistocene sediments were selectively eroded into residual quartz sand (Sombroek, 1990).

However, on the crystalline basement in Venezuela, the quartz sands of savanna-like Spodosol areas were found to be the weathering residues of local granite (Schnütgen and Bremer, 1985). Surprisingly, these savannas seem to be more widely distributed regionally on gneisses than on granites (Dubroeucq and Sanchez, 1981; Dubroeucq and Blancaneaux, 1987). Since present-day rain forests protect the ground from surface erosion and local runoff (Roche, 1981; Fritsch, 1992; Pimentel da Silva et al., 1992), the slope deposits and sandy sediments, on which Spodosols are presumably developed, were probably formed during Quaternary past dry periods (Tricard, 1974; Servant et al., 1981; Liu and Colinvaux, 1985; Lips and Duivenvoorden, 1994).

Nevertheless, in the Amazon basin, Oxisol–Spodosol associations are also described on a single landform unit and on a single parent material (Fritsch, 1984; Veillon, 1990; Dubroeucq et al., 1991) with close genetic links between the two soil types and without any lithogenic discontinuity (Turenne, 1975; Boulet et al., 1984; Lucas et al., 1987). Following the Oxisol to Spodosol transition along the slope, pronounced but progressive changes were observed in the distribution of major elements such as Si, Al, Fe and Ti (Chauvel et al., 1987; Lucas, 1989; Bravard and Righi, 1990). These changes are related to dissolution of clay minerals in the upslope Oxisols and Ultisols.

Results of analyses of rainwater, throughflow, surface runoff and groundwater, and experiments with bags of minerals inserted into the soil have shown that alternating dissolution and precipitation of kaolinite and oxihydroxides are active in Amazon soils (Grimaldi et al., 1994; Eyrolle, 1994; Cornu et al., 1995). This geochemical equilibrium between dissolution and precipitation is mainly controlled by the biological activity of the rain forest and by the hydrodynamics of the percolating water (Lucas et al., 1993;

Eyrolle et al., 1993). Where soil solutions slowly percolate vertically from the topsoil to deep subsoil, Si is mostly leached and Al and Fe are held back. Where topsoil drainage becomes lateral with a short residence time of the percolating waters, Fe, Al, organic colloids, and Si in a lesser proportion are leached, preserving only the stable minerals such as quartz (Lucas et al., 1996). The resulting kaolinite dissolution is a key process in soil transformation and could explain how Spodosols derive from clayey Oxisols.

Soil evolutions on tectonically stable continental shields are generally thought to result from climatic changes and/or isostatic variations. As observed in French Guyana, appreciable variations of the hydrostatic base level may generate secondary lateral or vertical differentiations into primary soils (Boulet et al., 1979). This is not specific to the Amazon basin (Thomas, 1994). In the Sahara and in southern California, Johnson (1985) has revealed that stability, subsidence or uplift episodes were related to changes in soil development and soil thickness. In general, modifications of the biogeochemical environment have been found to induce the formation of new horizons, whereas stability increases soil thickness (Hole, 1961).

Soil associations and soil sequences are good indicators of parent materials and soil forming processes, influenced by topography and climatic changes. To understand the soil evolution in the Rio Negro basin, a detailed examination of soil toposequences crossing representative landforms has been performed on crystalline parent rocks. We have placed a special focus on the structure and arrangement of the horizons from the topsoil to the saprolite.

2. Environmental settings

The Rio Negro basin extends from latitude 1°S to 4°N and from longitude 71°W to 66°W (Fig. 1). The climate is perhumid equatorial (Köppen = Afi). The mean annual temperature is about 26°C with differences of less than 5°C between the extreme monthly average temperatures. The annual rainfall ranges from 3000 to 4000 mm and the soil moisture regime (Soil Survey Staff, 1975, 1990) is udic to perudic in most of the area. There is no dry season, and a rainfall peak occurs during May and June. This maximum is more pronounced in the western and northern parts of the basin: Iauareté, San Carlos, Maroa. There is an excess of about 1000 to 2000 mm in the calculated annual water balance.

The geologic substratum is a Precambrian basement called the 'Complexe Guyanais' (Choubert, 1974) composed of migmatized and tectonized crystalline rocks ranging from feldspathic migmatites and gneissic granites to quartz-rich gneisses and micaschists. This basement is crossed by granite intrusions. The age of the different formations spans between 2900 and 2300 million years (Choubert, 1974; Cecilia Martin, 1976; Mendoza et al., 1977). Tectonized and metamorphic quartz-rich sediments are discordant upon this basement and appear locally as long and curved anticlinal ridges or asymmetrical round synclines. They are called 'Metasediments' (Mendoza et al., 1977) or 'Grupo Tunui' (Projeto Radambrasil, 1976) and estimated to be of the Precambrian-C period.

The entire region is a vast and level low plateau called 'Pediplano Rio Branco-Rio

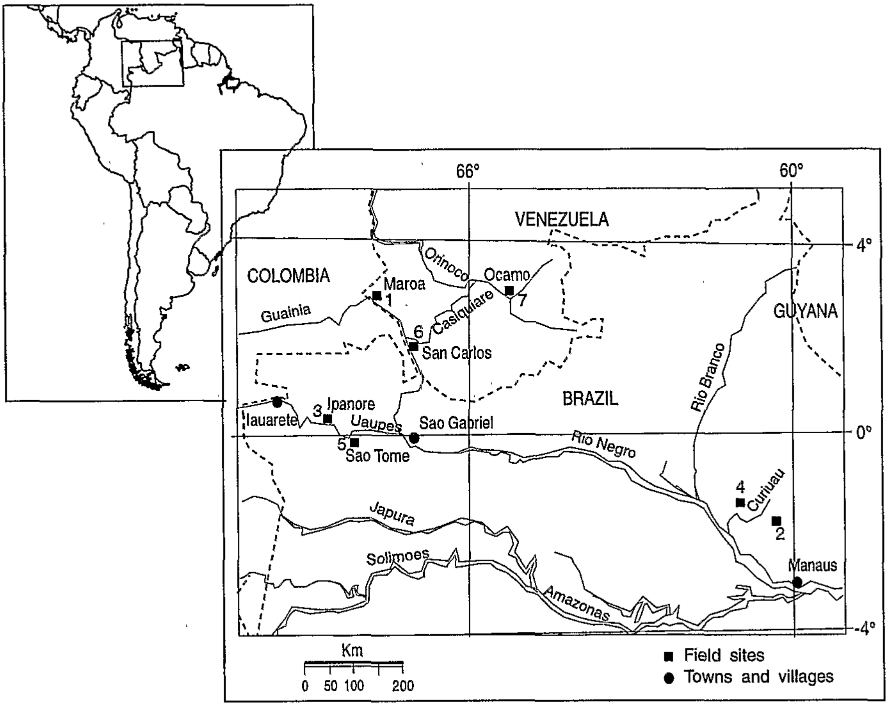

Fig. 1. Location map.

Negro' (Projeto Radambrasil, 1976), in which the only emerging reliefs are granitic inselbergs, quartzitic crests and fields of rolling convex hills.

3. Material and methods

3.1. The soil-geomorphic map

The primary aim of the present study was to extend to the whole basin the soil survey previously carried out in the Venezuelian Amazon region (Atlas del Inventario de Tierras del Territorio Federal Amazonas, 1987). For this purpose, several field trips in sites previously selected on Landsat and Radar-SLAR imagery at the scale 1:250,000 were conducted to the north of São Gabriel, along the Rio Uaupès, the Rio Iauíari and in the Rio Curiúau region. A reconnaissance map of the upper Rio Negro basin covering 165,000 km^2 at 1:500,000 has been drawn by coupling Radar-SLAR and Landsat images with field observations. The map units integrate topographic patterns and soil types in broad landscape subdivisions named soil-geomorphic units.

3.2. The soil-geomorphic units

The Rio Negro basin was divided into six broad map units dealing with soils, geomorphic levels and landforms. In the text, soil names in brackets refer to a standard classification (Soil Survey Staff, 1975, 1990).

3.2.1. The ferrallitic convex hills

This map unit is found on the highest sites of the basin. It consists of extensive fields of convex hills forming a multi-convex relief and assimilated as a geomorphic level named 'Lower multi-convex surface' (Gavaud et al., 1986). The altitude of the hill tops ranges from 95 to 160 m above sea level. The width of the hills varies from 400 to 800 m at the foot and from 10 to 20 m at the top, and elevations vary from 40 to 80 m. Narrow V-shaped valleys separate the hills. Red-yellow coloured Oxisols (Hapludox) are the predominant soils. The weathering mantle is generally very deep, particularly below the hilltop. Downhill the weathering mantle is shallower and outcrops of core boulders are frequent.

3.2.2. The low hills

This map unit shows an undulating landform composed of adjacent low hills, less than 30 m high, with flat tops and irregular contours. Narrow and flat valley bottoms separate the hills. Summit altitudes range from 80 to 130 m above sea level. Soils are yellow-red coloured Oxisols with a pebbly layer of concretions (Gibbsitic clayey-skeletal Hapludox).

3.2.3. The low hills with flat interzones

This map unit is composed of scattered hills 2 to 15 m high above a flat sandy inter-hill surface. Soils are concretionary, clay-poor Ultisols (Gibbsitic sandy-skeletal Kandiudults) on the hilltop and yellow-red coloured Oxisols with gibbsitic nodules or indurated blocks on the slope. Waterlogged Spodosols (Ultic Tropaquods) cover the whole inter-hill surface.

3.2.4. The ferrallitic plain

This map unit is a flat landform distributed mainly in the central and eastern parts of the basin, where general elevations range from 100 to 75 m above sea level. Compared with the hills, the soil mantle is relatively shallow above the bedrock. The prevailing soil is a clayey, yellow Oxisol (Humic Xanthic Acrudox), 2 to 3 m thick, rich in gibbsite and displaying thick, black epipedons. Beneath the soil mantle is the alterite, a 3 to 4 m thick sandy-clay matrix, containing essentially kaolinite, gibbsite, coarse quartz, muscovite and weathered feldspars in which core stones and boulders of crystalline rock are embedded.

3.2.5. The podzolic plain

This is the most extensive unit, widespread over the southwest part of the basin. The altitude of this low and very flat plain is 75 m above sea level in the middle of the basin, but it gradually reaches 120 m in the west and 90 m in the north of the basin. The podzolic plain is covered by non-stratified white sand, which corresponds to the albic horizon of giant Spodosols (Typic Quartzipsamments) in which a discontinuous hardpan, 0.1 to 2 m thick, composed of dark-brown layers of sand grains cemented by oxides and organic matter, is found at depths between 3 and 10 m.

3.2.6. The peat areas

Peat is found in the middle of the Spodosol areas. It is covered with a dense flood forest contrasting with the scarse evergreen bush on the Spodosols. Peat consists of a 30- to 80-cm thick organic mat, essentially composed of fine and medium roots and organic aggregates, floating on subsurface groundwaters. In the small flood forest areas, the peat blanket may be thick, and the prevalent soil is a Histosol. When the organic mat is less than 40 cm thick and the Spodosol is relatively shallow, the soil is a waterlogged Spodosol with peat (Histic Tropaquod). In the broad areas of flood forest, which stretch over the whole interfluve, the organic fibrous mat is thinner and peat soils alternate with bleached waterlogged Ultisols (Typic Albaquults).

3.3. Field sites and soil sequences

Seven sites have been selected and studied among the soil-geomorphic units (Fig. 1). They comprise six toposequences and one cut of a riverbank. In all the sequences, topography has been restituted from accurate field measurements. In three sequences, the horizonation of the soil mantle has been extrapolated from the successive pits and intermediate auger hole profiles. In the sections, pits are mentioned with letter F and augerings with letter S. For simplification, profile characteristics are given in Appendix A. Soils are represented by a sketch of their distinctive horizons.

3.4. Soils and horizons

To represent the soil mantle structure, special emphasis has been placed on horizon identification. Diagnostic horizons previously described in the Venezuelian Amazon region (Atlas del Inventario de Tierras del Territorio Federal Amazonas, 1987) served as a reference in the Rio Negro area. In this study, fifteen of them are used. Their principal descriptive field criteria are given in a glossary at the end of the text.

3.5. Sampling methods

Oriented undisturbed samples were taken from each horizon and conserved in sealed plastic boxes for impregnation. Sampling beneath the water in profiles with shallow groundwater was carried out by constant pumping during the digging. Disturbed samples for chemical and mineralogical analyses were taken out from the pits and from the augerings.

3.6. Optical, mineralogical and chemical analyses

Sixty-five soil thin sections were examined under an optical microscope with polarized and natural light devices, using the terminology of Bullock et al. (1985). Particle size distribution analyses of the < 2 mm soil fraction and heavy mineral identification were performed on 15 samples from several Oxisol and Spodosol profiles. Twenty-eight mineralogical analyses by X-ray diffraction using a Siemens D 500 diffractometer with Cu anticathode were carried out on the whole fraction and on the < 2 μm fraction.

Total chemical analyses have been performed using the 3-acid digestion method (Harrassowitz, 1926), which is supposed to solubilize the secondary minerals produced by weathering and preserve the primary minerals such as quartz and feldspars, and provides indications on the intensity of the weathering (Pédro, 1966). Semi-quantitative estimations of the abundance of mineral phases were calculated from the chemical composition of 3-acid digestion extracts and residues, and from peak heights or peak areas in X-ray diffractograms (Norrish and Taylor, 1962). In eight samples from Spodosols and their related Oxisols, selective chemical extractions of the various forms of Al, Fe and Si oxihydroxides were carried out. We used the acid–oxalate pH 3.2 reactive or Tamm (Blakemore, 1983), the dithionite–citrate–Na bicarbonate or DCB (Mehra and Jackson, 1960), the dithionite plus acid oxalate at 80°C (Hétier and Jeanroy, 1973) and the sodium–pyrophosphate reactive (Jeanroy, 1983). Al, Fe and Si contents of the extracts were quantified with an ICP (induced coupled plasma) SOPRA spectrometer. Muscovite grains and cryptocrystalline silica minerals from E horizons of giant Spodosols were separated by ultra-centrifugation and observed under a transmission electron microscope JEOL 100. These analyses were carried out in ORSTOM laboratories, Bondy, France.

4. Results

4.1. Sequence 1 in a ferrallitic convex hill

The soil mantle of the convex hills is quite continuous, and no clear soil changes appear along the hillside. The common profile is the yellow-red coloured Oxisol (Typic Hapludox). The lithologic heterogeneity observed in the saprolite disappears towards the surface. The residual poorly weatherable minerals in the soil are basically quartz, muscovite and K-feldspars (orthoclase) and the secondary minerals are kaolinite, gibbsite and aluminous goethite. On gneissic substratum, hydroxy-Al interlayered vermiculite is shown by XRD in the upper part of the soil (Table 1). Hematite is detected by XRD in the red saprolite and in the mottled saprolite horizons.

Table 1
Mineral phases in two different soils on ferrallitic convex hills, one on mica-rich gneiss and the other on feldspathic granite, estimated from XRD analyses and 3-acid digestion extracts and residues

Horizon	Pseudogley	Yellow oxic	Pale humic	Red oxic
Profile	Gneiss	Gneiss	Gneiss	Granite
Micas	+ +	+	0	0
Al-Vermiculite	0	+	+ +	0
Kaolinite	+ + + + +	+ + + + +	+ + + +	+ + + + +
Gibbsite	+ +	+ +	+ + + +	+ +
Al-Goethite	+	+	+	+
Rutile, Anatase	+	+	+	+

Intervals of values are 1–3 (+), 4–10 (+ +), 11–23 (+ + +), 24–28 (+ + + +) and 49–97 (+ + + + +) perc. of the < 2 μm soil fraction.

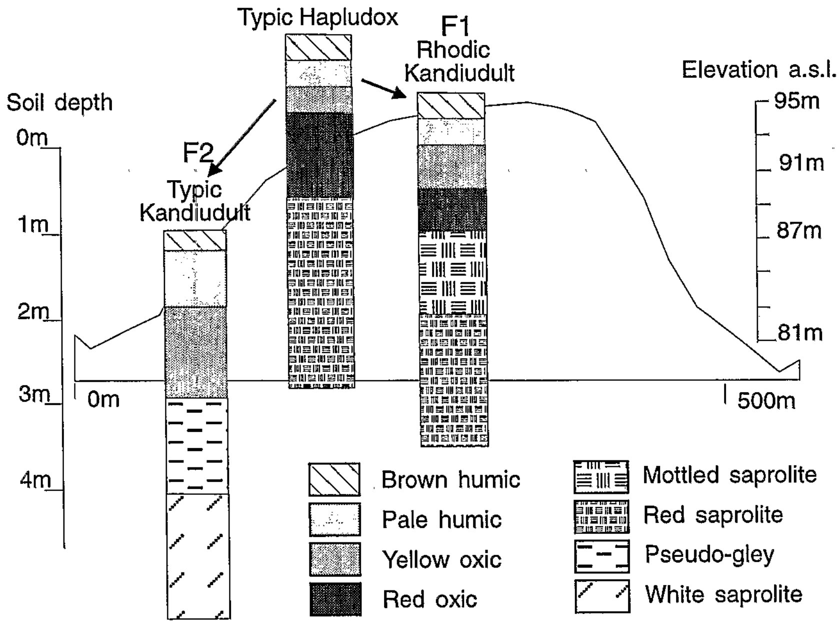

Fig. 2. Soil profile variation between summit and side of a convex ferralitic hill.

From top to bottom and limited to a depth of 4 m, the Typic Hapludox shows constantly the following horizons: brown humic–pale humic–yellow oxic–red oxic–red saprolite or regolith. Nevertheless, on a small convex hill of 14 m high in Maroa, Venezuela (Fig. 1, site 1), changes were observed upslope, such as the addition of a mottled saprolite above the red saprolite (Fig. 2, profile F1) and also downslope, such as white saprolite instead of red saprolite and pseudogley instead of red oxic horizons (Fig. 2, profile F2).

4.2. Sequence 2 in a low hill

Along a hillside on gneissic granite with two mica types, 3 km to the west of a position 157 km from Manaus on the Manaus–Boa Vista road, Brazil (Fig. 1, site 2), the following sequence is observed (Fig. 3): uphill a yellow-red Oxisol with concretionary layer (gibbsitic clayey-skeletal Hapludox, profile F3), concretions are gibbsitic (gibbsite > 70%) and the mineral composition of the fine fraction is similar to that of the soil on convex hills; on the slope, a red Oxisol (Typic Hapludox, profile F6); downslope a yellow Ultisol (Plinthic Kandiaquult, profile F4); at the footslope, a hydromorphic Ultisol with a bleached horizon (Typic Albaquult, S3 in the sequence). We did not find any Spodosols in the zone, nor around the neighbouring hills.

The cross-section of this sequence shows two contrasted domains. In the upslope domain, which extends from the top to the lower third part of the slope, the horizon boundaries are widely convex and oriented vertically downwards. In the downslope domain, horizons are waving tongues. Their extremities are oriented towards the top of the hill. This disposition could easily be interpreted as successive slope deposits on the

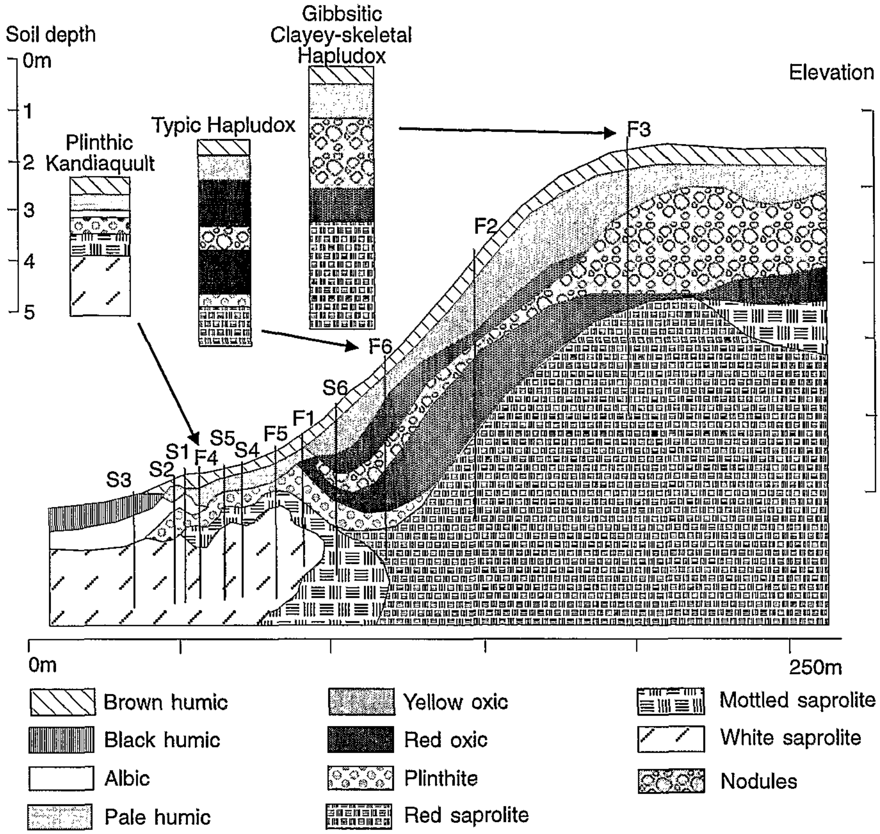

Fig. 3. Cross-section of a hillside without Spodosol. The soil mantle is divided in two domains. In the upper domain, the horizons are parallel to the soil surface, and their extremity is widely convex and oriented downwards. In the lower domain, the horizons are found in waving tongues with their extremity oriented towards the top of the hill.

hillside and lateral sand and clay admixtures downslope. But, despite this contrasted aspect, continuous transitions exist between adjacent soils.

Results from particle-size analysis and oxide extractions show a gradual loss of clay along the slope with a correlative increase of the sand fraction except in the white saprolite horizon, in which an increase of clay in relation to the adjacent horizons is noticed (Fig. 4). In the whole soil mantle, a progressive loss in DCB-extractable Fe and Al oxides is observed from upslope to downslope. The marked increase in Fe–Tamm/Fe–DCB ratios in the inferior part of the sequence (Fig. 4) signifies that crystalline forms of Fe-oxides change to non-crystalline forms, downslope where aquic conditions prevail. Furthermore, continuous transitions were also observed between adjacent horizons.

From the red oxic horizon to the yellow oxic horizon, the quartz grains change gradually in shape and size. They become smaller and smoother with some secondary overgrowths of amorphous silica and dissolution alveoles. These features show undoubt-

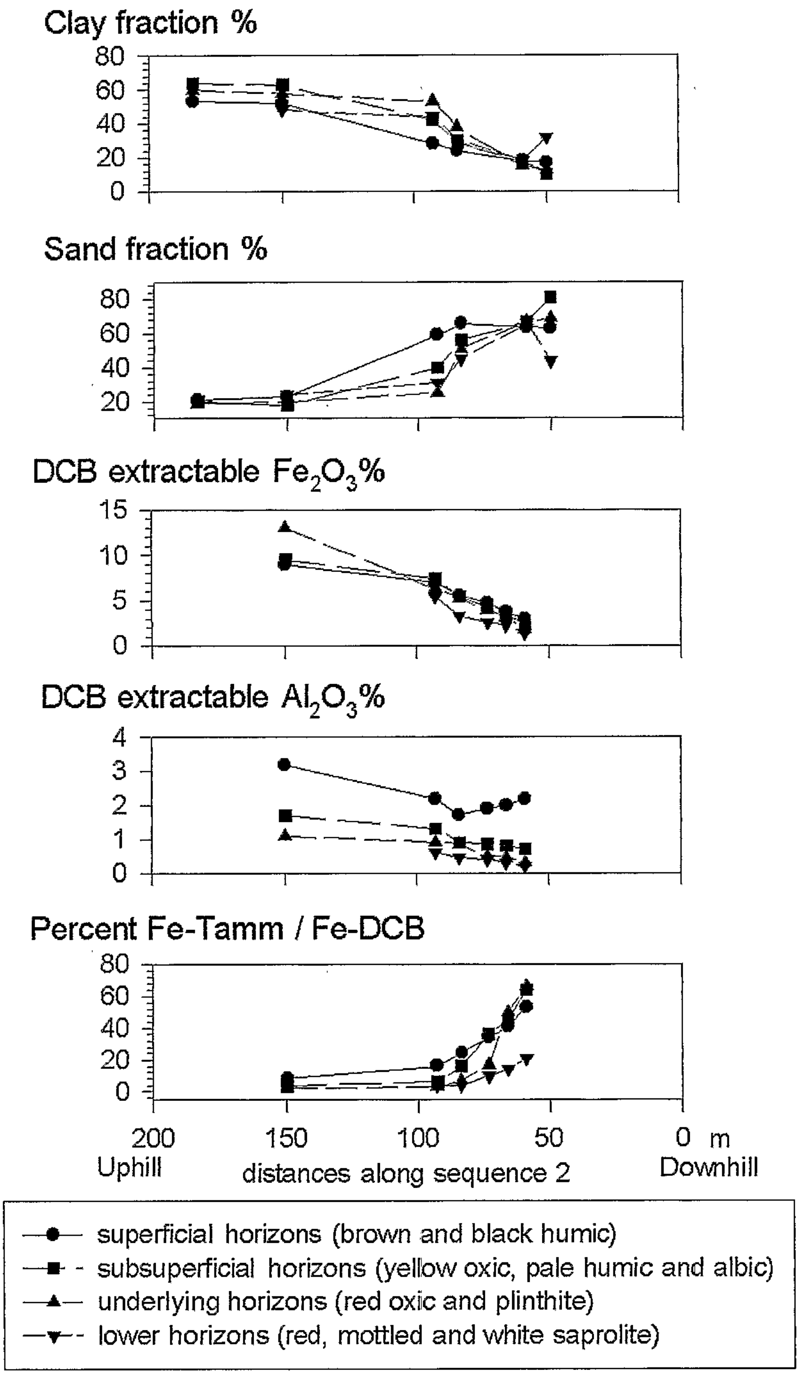
Clay fraction %
80
60
40
20
0
Sand fraction %
80
60
40
20
DCB extractable Fe_2O_3%
15
10
5
0
DCB extractable Al_2O_3%
4
3
2
1
0
Percent Fe-Tamm / Fe-DCB
80
60
40
20
0
200
150
100
50
0 m
Uphill
distances along sequence 2
Downhill
superficial horizons (brown and black humic)
subsuperficial horizons (yellow oxic, pale humic and albic)
underlying horizons (red oxic and plinthite)
lower horizons (red, mottled and white saprolite)

edly a chemical erosion rather than a physical abrasion due to transport. Downslope, the yellow oxic horizon is thinner (Fig. 3), and the texture gradually changes to sandy-loam (pale humic horizon) and then to pure sand (albic horizon). Microscope observation show that quartz grains keep the same aspect throughout the yellow oxic, the pale humic, and the albic horizons. This probably means that the quartz grains of these three horizons have the same authigenic origin and are all issued from the red oxic horizon, which is contrary to the hypothesis of admixtures of albic sand in the valley bottom by fluvial transport.

By microscope observation, another relationship can be established between the red saprolite, the mottled saprolite and the white saprolite. The mottles are red (Munsell 10R3/4) and show a stippled-speckled birefringent plasma, which is identical to the plasma of the red saprolite. Therefore, the mottles can be considered as remnants, or pedorelicts, of a former red saprolite horizon. In the white saprolite, deep alveolar dissolution cavities are observed on the quartz grains, as well as centimeter-large light grey coloured areas with undifferentiated b-fabric, which are domains of randomly arranged fine particles of neoformed clay. These micromorphologic features are indicators of an important quartz dissolution and a significant kaolinite neoformation. They also suggest that, through the effects of quartz dissolution and kaolinite neoformation, the white saprolite can differentiate from the mottled saprolite and, through the effects of iron oxide depletion, the mottled saprolite can differentiate from the red saprolite.

The red oxic horizon is directly followed downwards by the plinthite horizon. Micromorphological observations reveal that the same cross-striated birefringent fabric is observed both in the red oxic horizon and in the mottles of the plinthite. This fabric is mainly composed of kaolinite and gibbsite with aluminous goethite. The red-brown mottles should be thus considered as pedorelicts of red oxic horizon rather than intrinsic Fe concentrations. Therefore, the thin plinthite horizon, downslope in the sequence between the albic horizon and the white saprolite (Fig. 3), could well have been, formerly, a red oxic horizon.

Analytical data, macro- and micromorphological observations do not show any lithologic discontinuity. On the contrary, they indicate that the contrasted sequence of red Oxisols, uphill and bleached Ultisols, downhill, should have normally and gradually developed from a single parent material derived from the weathered gneissic granite basement.

4.3. Sequence 3 in a low hill surrounded by flat sandy areas

The sequence is on granite, near Ipanore, Brazil (Fig. 1 site 3). It consists, upslope to downslope (Fig. 5), of a mottled Oxisol (Plinthic Kandiudox, profile F1), a bleached Ultisol (Arenic Umbric Kandiaquult, profile F2) and a waterlogged Spodosol (Ultic Tropaquod, profile F3).

Fig. 4. Particle-size analysis and oxide extractions from sequence 2 show a gradual loss of clay along the slope, except in the white saprolite where clay content increases. Downslope, important but progressive Fe and Al losses are noticed. The increasing values of Fe–Tamm/Fe–DCB ratio indicate that crystalline forms of Fe oxides change to non-crystalline forms downslope.

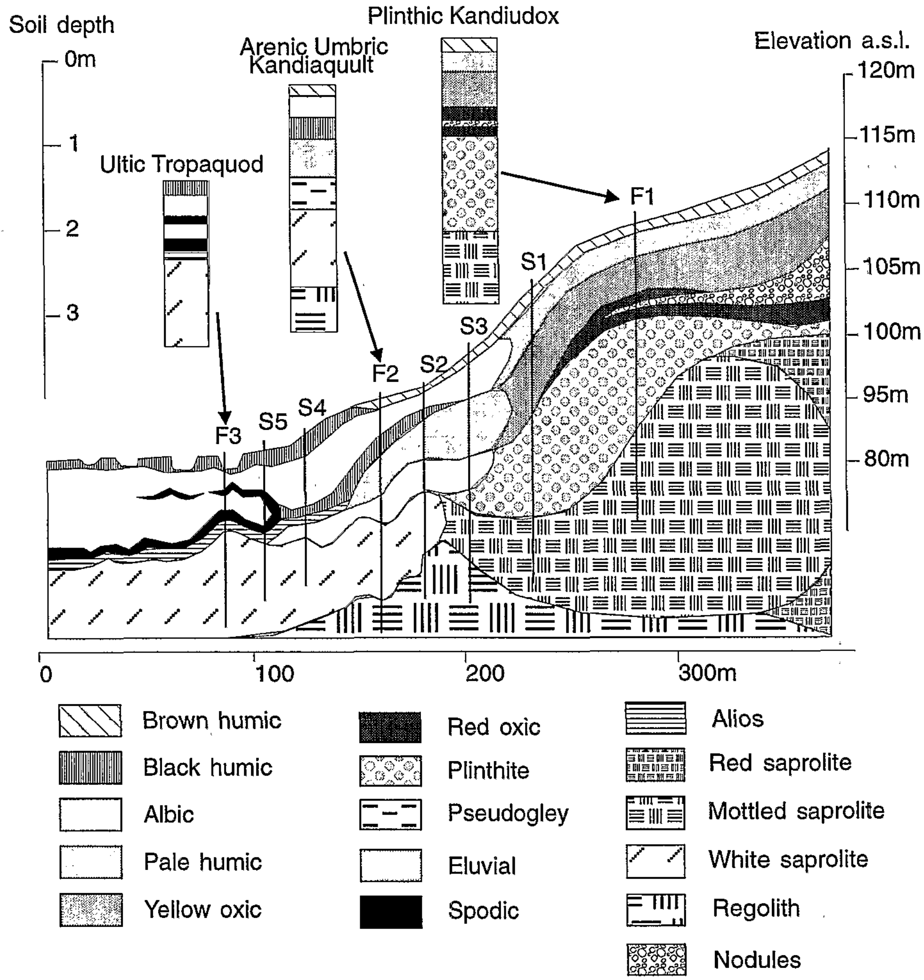

Fig. 5. Cross-section of a hillside with Spodosol downslope. The albic horizon penetrates directly upward into the Oxisol domain. The limit between Ultisols and Spodosols is marked downslope by surficial microreliefs in connecting channels and hollows.

The cross-section (Fig. 5) shows a prominent branch of albic horizon, oriented upslope, and another smaller branch, oriented downwards and surrounded by an aureola of black spodic horizon. Downslope, near the valley floor, a thin alios horizon (Bs) separates the spodic horizon (Bh) from the underlying white saprolite.

This disposition could be interpreted as lateral deposition of sand in the valley by flood waters. However, identification of heavy minerals in the Oxisol and the Ultisol profiles show the same granite parentage, except deep in the Ultisol where metamorphic influences are probable (Table 2).

Mineralogical and micromorphological observations indicate that the black humic horizon in the Ultisol and the spodic horizon in the Spodosol have many similarities.

Table 2
Heavy mineral distribution in Oxisol F1 and Ultisol F2 profiles from sequence 3

Sequence 3	Profile F1			Profile F2			
Horizons	Pale humic	Yellow oxic	Plinthite	Albic	Pseudo gley	White saprolite	Regolith
Granite minerals							
Fresh zircons	23	48	87	21	53	34	20
Corroded zircons	44	42	0	35	0	23	0
Turmaline	1	0	0	1	0.5	5	0.5
Anatase	0	0	0	0	0	0	0
Brookite	1	1	0	0	0	0	0
Monazite	2	0.5	0	1	0.5	0	0
Metamorphic minerals							
Andalusite	2	1	0	1	0	5	10
Staurolite	0	0	5	0	1	0	0.5
Sillimanite	0	0	0	0	0.5	3	0
Kyanite	0	0	0	0	0.5	3	11
Corundum	0	0	0	0	0	0	0
Abraded subrounded minerals							
Zircon	0	0	0	1	1	6	0
Turmaline	1	1	0	0	0	0	19
Ubiquitous minerals							
Rutile	4	0.5	0	4	9	9	30
Epidote–zoisite	22	5	8	18	13	7	10
Undif. weathered min.	0	2	0	12	23	5	0

The two soils show a predominantly granitic influence, except in the Ultisol, where metamorphic influences and high proportion of abraded zircons appear below a depth of 3 m.
Probable lithologic contact and intense corrosion by groundwater flows should explain these results.
No evidence of fluvial deposit is noticed in the subsurface horizon of Ultisol F2.

Both are composed of coarse quartz grains with dark-brown microaggregates of 0.10 to 0.15 mm in size, mostly capping the grains. This fine material is basically composed of microquartz, organic matter, small amounts of kaolinite with Fe and Al oxides, and relatively large amounts of titanium oxides (rutile, anatase).

Other similarities can be found between the yellow oxic horizon of the Oxisol, the eluvial horizon of the Ultisol, and the alios horizon of the Spodosol.

(1) The eluvial horizon has a bridged grain structure. The pellicles and bridges of fine material between the coarse grains are nonbirefringent and without cutans of redistributed material. They show the same aspect under the microscope and the same global mineral composition by XRD analysis as the fine matrix of the yellow oxic horizon (microcrystalline gibbsite, kaolinite, Al-goethite), but they are richer in Al and Fe oxides. This suggests that the eluvial horizon was probably a former yellow oxic horizon, which have been submitted to an important clay depletion relative to oxides and quartz.

(2) The alios horizon has an intergrain microaggregate structure. The fine material is red-brown, isotropic, with curved retraction cracks, and more abundant than in the

Table 3
SiO_2, Fe_2O_3 and Al_2O_3 contents in different extracts from the 'spodic' (Bh) and 'alios' (Bs) horizons of a waterlogged Spodosol (Ultic Tropaquod), in percent of the < 2 μm soil fraction

Extract	Horizon	SiO_2	Fe_2O_3	Al_2O_3
Tamm	Bh	0.00	0.06	0.15
	Bs	0.06	0.10	1.10
Dithionite + oxalate	Bh	0.00	0.06	0.134
	Bs	0.00	0.12	1.05
Pyrophosphate	Bh	0.06	0.01	0.15
	Bs	0.43 *	0.02	1.50 *

The exaggerated values marked by * are due to particles of dispersed clay.

eluvial horizon. Gibbsite and kaolinite are found here as they were in the eluvial horizon but, in the alios, the global iron content decreases and that of aluminium and amorphous minerals increases: dithionite + oxalate extractable Fe oxide is only 0.12%; Al oxide is 1.05% (Table 3); one can find here only traces of aluminous goethite, although it is clearly evidenced by XRD in the oxic horizon.

In the subsoil, the red-brown mottles of the plinthite and the yellow mottles of the pseudogley horizon show the same porostriated birefringent iron-clay fabric. This provides another micromorphological resemblance and a probable genetical link between two consecutive horizons.

Trends of horizon orientations and the persistence of some pedological features in adjacent horizons may be indicators of a lateral evolution of the soil mantle (Boulet et al., 1982; Fritsch et al., 1992). The horizonation in sequence 3 could therefore be also interpreted as the result of the active intrusion of the albic horizon into the Oxisol domain, rather than admixtures of sand on the valley floor by stream flow deposits.

Downhill, microreliefs of connecting channels and hollows develop just above the small tongue of albic horizon that is oriented downwards (Fig. 5). These microreliefs could, at first glance, be interpreted as abandoned stream channels. However, they could be also interpreted as surficial collectors of the excess of water draining from the hill to the valley floor through the albic horizons.

4.4. Sequence 4 in a ferrallitic plain

This sequence is on granite in the Rio Curiúau region, an affluent of the Lower Rio Negro (Fig. 1 site 4). It develops along very gentle slopes with an elevation of 2.5 m only and along a short distance of 80 m. Upslope to downslope (Fig. 6) the main profiles are: yellow Oxisol (Xanthic Acrudox, profile S5), mottled Ultisol (Plinthic Kandiudult, profile F2), bleached Ultisol with a compact albic horizon (Aeric Albaquult, profile S4), and finally waterlogged Spodosol (Aeric GrossarenicTropaquod, profile F5).

Upslope in the section (Fig. 6), the pale humic, yellow oxic and plinthite horizons are parallel to the ground surface. Downslope, the yellow oxic and the pale humic horizons abruptly disappear into an albic horizon forming a gap in the soil mantle structure. This

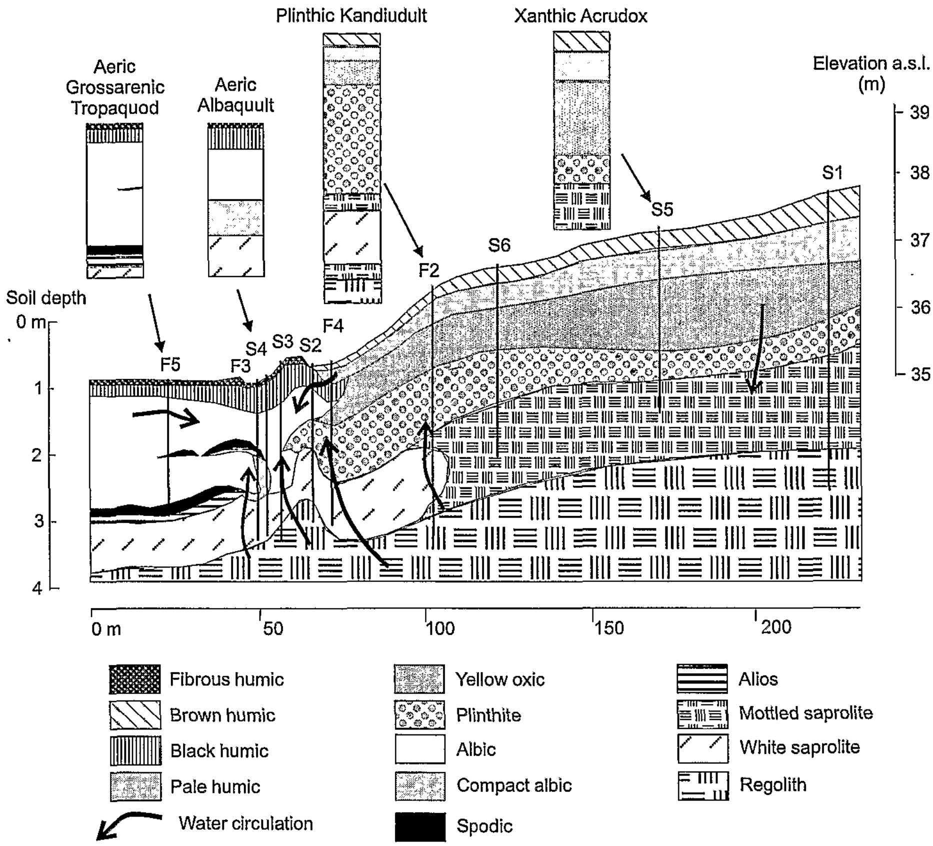

Fig. 6. Cross-section in the ferrallitic plain. Arrows figure the direction of the groundwater flow. All the fluxes meet at the extremity of the albic horizon. The groundwater stored within the regolith horizon flows up through the massive white saprolite horizon by means of natural pipe drains.

horizonation could be interpreted as a cut-and-fill sequence of sedimentation; but the albic horizon is not a simple sand bed. It is divided into two branches, the main branch is several meters long and oriented towards the Oxisol and the small branch is pointing down. The white saprolite also penetrates about 20 m into the Oxisol domain.

Like sequence 3, this sequence can be interpreted as a single catena developed on a single parent material.

Digging below the groundwater level under constant pumping has provided precious field observations on the way the water circulates within the soil. In the Ultisol profiles, the flux of water is oriented from the bottom to the surface. The groundwater under pressure is drained upward through various natural pipes of about 5 cm in diameter and 1 m in length. Totally hollow, they cross vertically the clayey white saprolite and liberate springs of water into the plinthite and the albic horizons (Fig. 6). In the Spodosol domain, downslope, the groundwater is subsuperficial and circulates upon the alios. These observations, together with measurements of the groundwater levels in the Oxisols, lead to the following explanation.

The high permeability in Oxisols enhances vertical infiltration. The groundwater is stored inside the deep regolith horizon and is retained in the Oxisol compartment by means of the white saprolite horizon, which is like a clay stopper to the lateral drainage. Theoretically, at this point of the sequence, the water circulation should be blocked, but the natural pipes facilitate the passage of the water under pressure through the clay stopper. Therefore, the descending tongue of the albic horizon corresponds to the path along which the upwelling groundwater arises to the soil surface. The surficial channels are vertically related to the extremities of the albic horizons and constitute natural outlets for the drainage water surplus.

The white saprolite horizon exhibits a prominent rise above a similar rise of the deep regolith horizon (Fig. 6). It could be related to the structure of the bedrock; but it could be also a channel of upwelling groundwater within the regolith horizon.

Another important point is the formation of a compact albic horizon in the downslope Ultisols (profiles S4 and F3) which is constituted of corroded quartz grains with deep dissolution pits, coalescent microquartz and brown amorphous organic coatings (Fig. 7). Loam- and silt-sized microquartz grains result from the corrosion of coarser grains that are found in sites where the drainage flow is particularly important (Lucas, 1989; Bravard and Righi, 1990). They form a secondary silty-loam fabric that clogs the intergrain porosity. At this point of intense lateral drainage, this fabric works like a filter, and the organic matter in suspension is trapped in the compact horizon. This pedologic feature is undoubtedly the first step in the development of a spodic horizon. Spodic and alios horizons are effectively observed just a few meters downslope in the sequence.

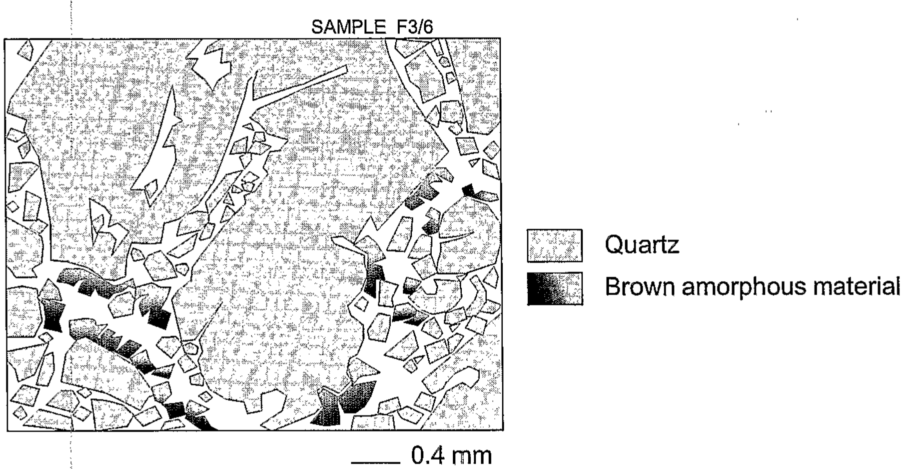

Fig. 7. Thin soil section of profile F3 in sequence no. 4. The compact horizon observed between depths of 160 and 180 cm is composed of intensely corroded quartz grains with deep dissolution pits, abundant microquartz and isotropic pale brown coatings with contraction cracks due to dehydration. The thicker coatings exhibit a laminated structure in PPL, without birefringent fringes in XPL.

4.5. *Sequence 5 in a podzolic plain*

On Precambrian gneissic granite at São Tomé, Uaupès, Brazil (Fig. 1, site 5), small patches of Histosols are scattered among giant Spodosols (Quartzipsamments). In this sequence (Fig. 8), differences in the vegetation are closely related to soil changes: Histosols sustain a flood forest with tall trees but giant Spodosols, in which the groundwater level is much deeper, sustain only a low sclerophyllous bush.

The Histosol profile (Hydric Tropofibrist, profile F1) consists of a surficial fibrous mat of live and decayed roots with humified organic matter upon waterlogged humic and argillic horizons between depths of 0.5 and 1.5 m (Fig. 8).

Peat profiles gradually develop into giant Spodosol profiles (Typic Quartzipsamments) where the groundwater is shallow. The differentiation begins with the formation of a compact albic horizon, made up of corroded quartz grains embedded in a loose crystallitic b-fabric of residual microquartz. Below the compact albic horizon, a secondary argillic horizon of sandy-loam or even sandy-clay-loam texture is found. The fine material is mainly composed of microquartz and a lesser proportion of vermiculite and kaolinite clay minerals, forming with the coarse quartz grains an intergrain microaggregate structure. Microquartz is a residue of the fragmentation of quartz grains. Clay is a product of the alteration of fine muscovite and orthoclase minerals in the albic horizon of the giant Spodosols (Dubroeucq and Volkoff, 1988). The compact albic and underlying argillic horizons operate like a filter, retaining the organic matter from the forest litterfall and thus forming a thin spodic horizon (Fig. 8, profiles F1 and F2).

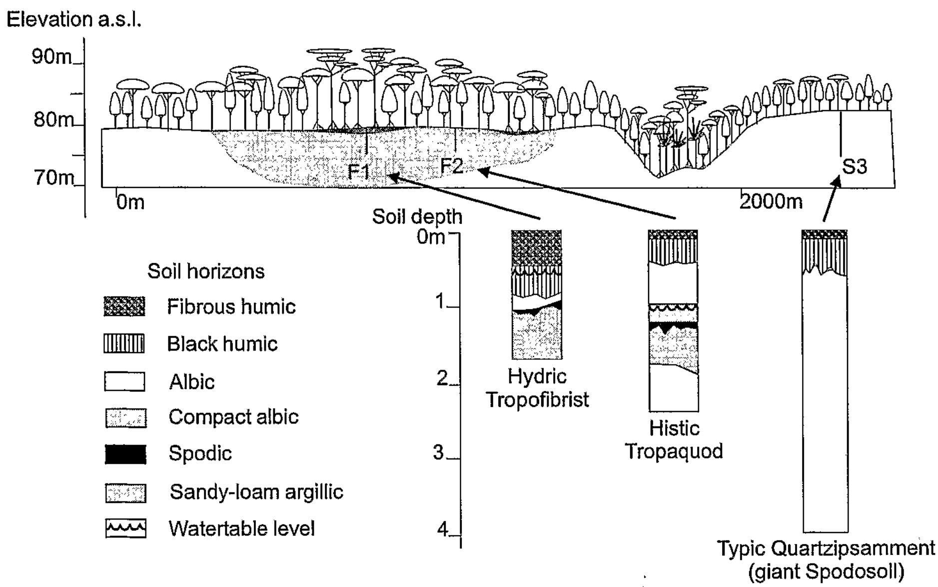

Fig. 8. Cross-section of a low plateau with giant Spodosols and Histosols. Histosol profile consists of surficial fibrous and black humic horizons overlying shallow spodic and argillic horizons. The argillic horizon differentiates into the giant Spodosol when the groundwater rises near the soil surface. Subsuperficial spodic and argillic horizons act as barrier retaining water and organic matter at the soil surface.

Peat is generally found near the middle of the broad interfluves of the podzolic plain. It is considered as the result of a secondary episode of weathering in the giant Spodosols, caused by a general rise of the groundwater level (Volkoff et al., 1990), which is probably the consequence of a wetter climate in this region.

4.6. Sequence 6 in a peat area

Relationships between Histosols and waterlogged Ultisols are shown in a catena on the granite basement at San Carlos de Rio Negro, Venezuela (Fig. 1, site 6). The sequence crosses a smooth flood depression in a sandy plain covered with Spodosols. This plain, overgrown with a savanna-like vegetation, is surrounded by contrasting Oxisols with dense rain forest cover and outcrops of core boulders (Fig. 9). From the sandy plain to the depression, profiles are the following: hydromorphic Spodosol (Aeric Grossarenic Tropaquod), peaty Spodosol (Histic Tropaquod), bleached Ultisol (Arenic Kandiaquult) and waterlogged Ultisol (Typic Albaquult). The difference in elevation between the peripherial Histosol and the central Albaquult is about 3 m.

Due to the lack of intermediate augerings, the horizonation of the soil mantle has not been extrapolated. However, differences between the profiles are evident. From the outer part to the center of the depressed area, the thickness of both fibric and sombric horizons

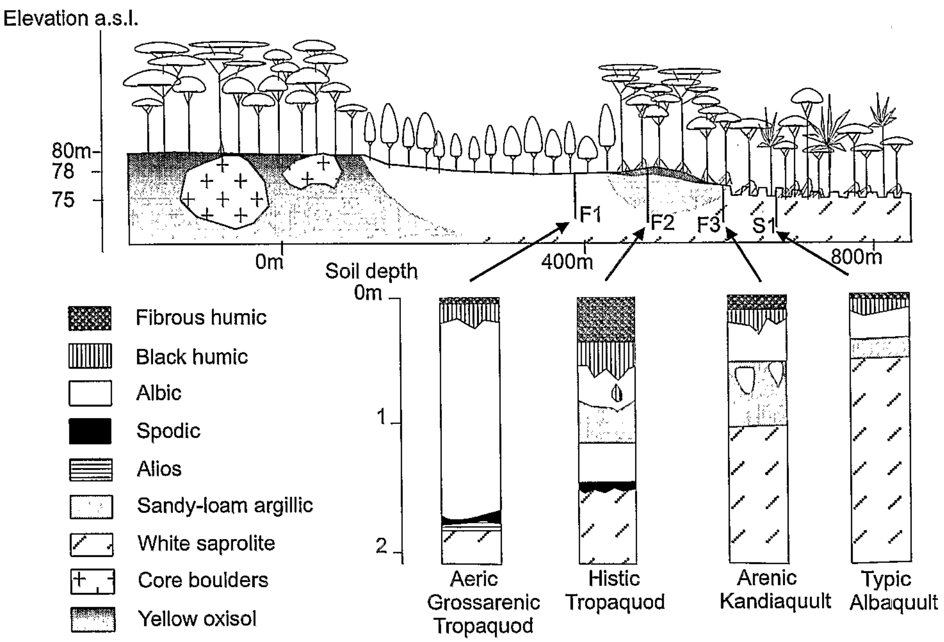

Fig. 9. Cross-section of a depressed area with waterlogged Ultisols amidst a broad area of Spodosols. From the periphery to the center of the depressed area, fibric and sombric horizons thin out, the argillic horizon disappears and, finally, the thickness of the sandy mantle decreases.

decreases gradually, the albic horizon thins out, and the secondary sandy-loam argillic horizon disappears. From the Spodosol to the bleached Ultisol, the sand cover loses 1.7 m in thickness and the upper boundary of the white saprolite deepens by 1.3 m in relation to the ground surface.

5. Interpretation and discussion

5.1. The Oxisol–Spodosol transformation

The Rio Negro sequences provide information additional to other Oxisol–Spodosol studies from Central Amazonia on Tertiary sedimentary formations (Lucas, 1989), from French Guyana on Quaternary sediments (Turenne, 1975), and on crystalline Precambrian shield (Fritsch et al., 1986; Veillon, 1990). This sum of information lead us to admit that, in various geologic and topographic situations, Spodosols, Ultisols and Oxisols can be found simultaneously on the same parent material. In the Rio Negro basin, either on the hillsides or in the ferrallitic plain on crystalline basement, Spodosols are associated with Ultisols and Oxisols (sequences 3 and 4). Three causes to this soil distribution are equally probable: (i) coarse sediments occur between the hills, (ii) colluvium has been transferred from upslope and, (iii) progressive transformation of the Oxisols into Spodosols is taking place.

Nobody has found, so far, an undisputable explanation for this soil distribution. However, in the sequences studied, Spodosols can be considered as the result of the Oxisol transformation rather than soil formation from fluvial sediments or slope deposits. The transformation process involves gradual clay depletion and oxide removal, which opens the way to Spodosol differentiation. The mechanisms at the beginning of the clay depletion should be the acidic hydrolysis of clay minerals by the soil solutions. The low pH is mainly controlled by the velocity of the organic matter decomposition, the forest cation uptake and the CO_2 production by root respiration (Berthelin et al., 1990; Grimaldi and Pédro, 1996). Nevertheless, the process of clay depletion within the soil is not yet clear. The sequences show that the process takes place only when the parent Oxisol mantle is already differentiated into yellow oxic, plinthite, mottled and white saprolite horizons. Both yellow oxic and plinthite horizons are then bleached into a white sandy material, and this active leaching is induced by the lateral drainage and the upwelling of the groundwater to the soil surface. From a geomorphic viewpoint, these processes are of upmost importance to the chemical erosion of the landscape (Thomas, 1994).

In the hilly landform, the Spodosol development leads to the regressive erosion of the hillside with global reduction of the dimensions of the hill. Consequently, the interhill surface widens, and a flat sandy surface is formed between scattered ferrallitic mounds as remnants of the hills (Fig. 10). This type of landscape is characteristic of broad areas surrounding the podzolic plain in the Amazon Territory of Venezuela (Atlas del Inventario de Tierras del Territorio Federal Amazonas, 1987).

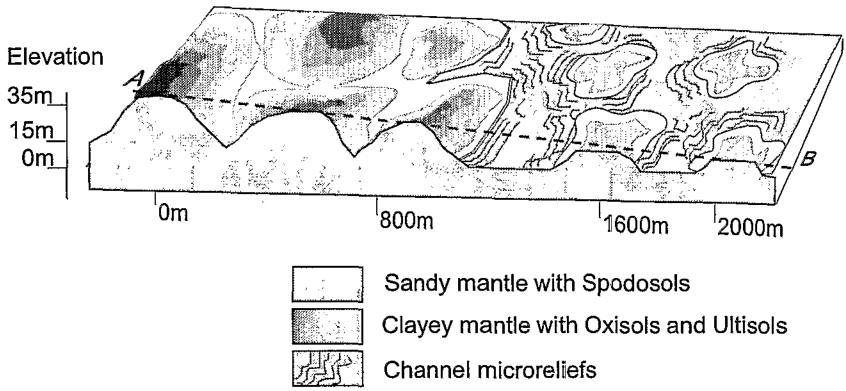

Fig. 10. Topographic diagram from an enlargement of the Radar-SLAR imagery, south of Santa Barbara, Orinoco, Venezuela. The limit between the two hilly landforms, one without Spodosols and the other with flat areas of Spodosols, is rather a transition than a contact.

In the ferrallitic plain, Spodosols develop generally at the edge and near the center of the Oxisol areas and generate a secondary low and flat sandy surface at the expense of the smooth landform covered with yellow Oxisols.

5.2. The hill transformation

Field and micromorphological observations of soil profiles in the hilly landscape have not revealed any important sediment transport nor any slope deposits. This is probably due to the chemical mobility and translocation of elements through the weathering profile, that are more predominant in wet tropical terrain under primary rain forest than in arid tropical terrain (Thornber, 1992). Field experiments have confirmed that particle transport and local runoff remain very low under rain forest, compared to chemical weathering and internal drainage (Roche, 1981; Fritsch, 1992; Pimentel da Silva et al., 1992).

In the initial yellow-red Oxisols of the convex hills, transformation processes seem to induce gradual changes in the soil mantle (Figs. 2 and 3). In a context of chemical erosion and changes in soil volume, intense clay and oxide removal along the hillside could lead to profile thinning, and the moderate clay neoformation in the white saprolite at the footslope could tend to profile preservation (Johnson, 1985). This differential geochemical evolution between the hillside and the hill summit presumably causes the regressive erosion of the hillside towards the hill centre, the development of a gentle slope at the foothill and, on the hill summit, the progressive sinking of the soil profile into the weathering zone. Consequently, the hill should become lower, flatter, and its circumference should shorten.

A three-stage evolution scheme was proposed from similar soil sequences in French Guyana by Veillon (1990). In the first stage (Fig. 11), a yellow oxic horizon develops from the red oxic horizon at the top and the sides of the hill and, on the hillside, a white saprolite develops from the red saprolite. In the second stage, on the hill summit, a

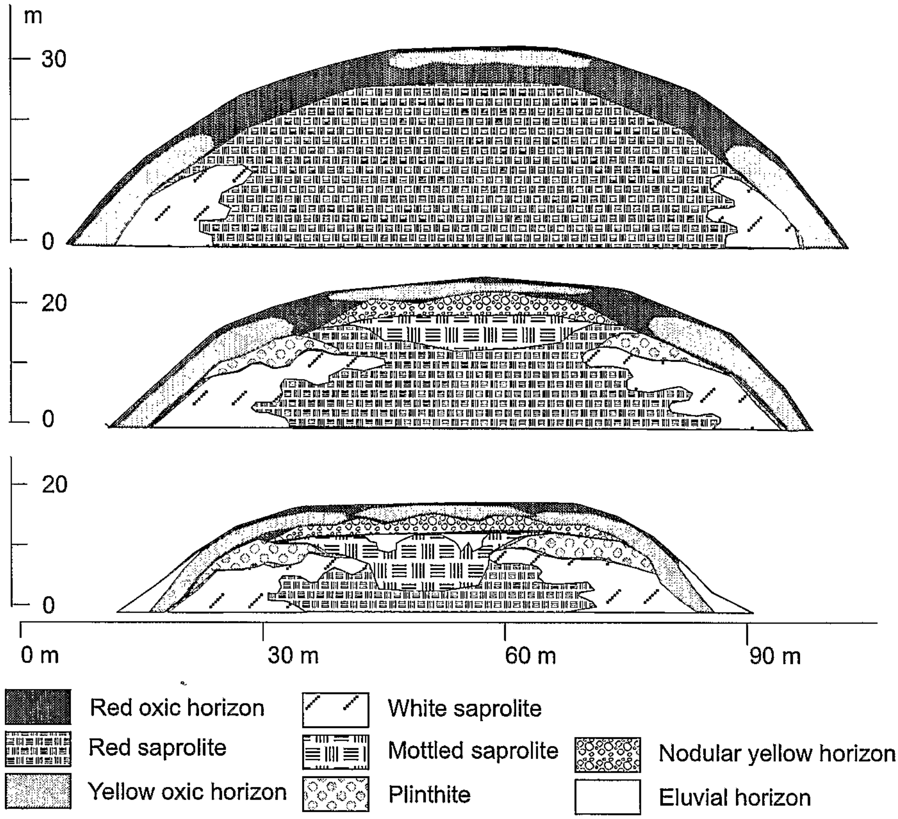

Fig. 11. Sketch of evolution of a ferrallitic hill: In the initial stage a yellow oxic horizon develops from the red oxic horizon and the red saprolite is transformed into a white saprolite downslope. In the second stage, a nodule layer differentiates from the red oxic horizon and a mottled saprolite differentiates from the red saprolite on the hilltop, and a plinthite differentiates from the red oxic horizon on the slopes. In the third stage, when the soil water regime becomes seasonally saturated, a network of albic and eluviated horizons develops on the summit and downslope. At every stage of evolution, the hill becomes lower and flatter and its circumference decreases.

concretionary layer differentiates from the red oxic horizon and a mottled saprolite differentiates from the red saprolite; on the hillside, a plinthite underlies the red oxic horizon. In the third stage, when the soil water regime periodically gets saturated on the flat top of the hill, a drainage network of albic and eluvial horizons develops both at the center (Veillon, 1990) and on the slopes of the hill. At each stage of evolution, the size of the hill decreases.

Equivalent transformations were described in French Guyana and Central Amazonia (Fritsch et al., 1986; Lucas, 1989) and were supposed to result from drainage changes in the pedologic cover under a general rise of the groundwater level, due to either a durable increase of the annual rainfall or the subsidence of the area (Boulet et al., 1979; Blancaneaux, 1985).

5.3. The Spodosol transformation

Peat and hydromorphic soils (Histosols and Albaquults) sustaining a dense flood forest amidst the podzolic plain may be interpreted as secondary soils developed in primary Spodosols. The intense dissolution and microfragmentation of the quartz grains, the cementation of the fine grains by organic particles, and the weathering of residual muscovite and orthoclase minerals, are all evidences of a soil transforming process that can be interpreted as follows (Fig. 12).

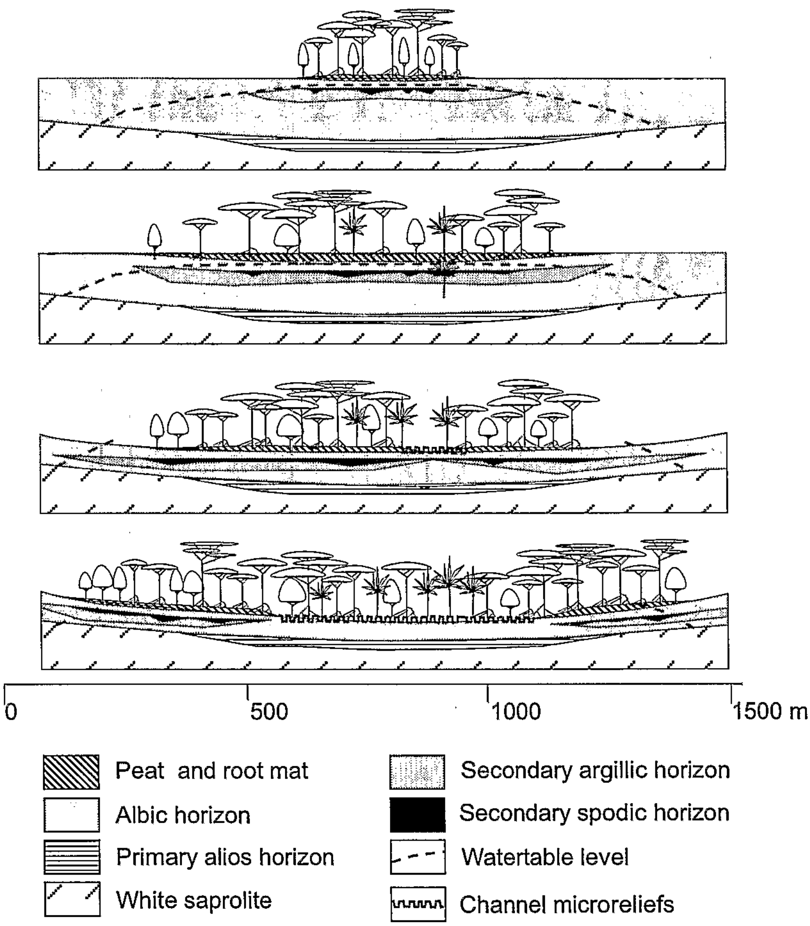

Fig. 12. Sketch of evolution of the podzol plain. In small zones, where the groundwater rises to the surface, secondary compact albic and argillic horizons develop within the bleached horizon of the giant Spodosol. Under the effects of shallow groundwater and the forest vegetation a secondary spodic horizon develops, inducing a subsuperficial expansion of the groundwater. Quartz dissolution increases and, consequently, the sandy mantle gets thinner. The result is the lowering of the area and the generalization of the microreliefs as outlets of surficial water surplus.

The process occurs near the center of the Spodosol plateau where the groundwater rises to the soil surface. A compact subsuperficial horizon develops by microfragmentation of the quartz grains and retains water and organic matter and favours the vegetation growth. The organic residues produced by the biomass clog the porosity of the compact albic horizon and form a new spodic horizon. In a more advanced stage of evolution, this horizon expands laterally and the groundwater spreads superficially because, as a result of quartz dissolution, the sandy mantle becomes thinner. A surface network of connecting channels drains the water excess. At this point of evolution, the organic matter is leached to the rivers, Histosols are degraded, and quartz dissolution increases.

This process has direct consequences in the landscape evolution: the flood depressions in the middle of the Spodosol areas, with their network of surficial channels acting as diffuse drainage axis, lead gradually to the thinning of the sandy mantle and the general erosion of the low plateau. This erosion is achieved when waterlogged Ultisols are developed directly upon the white saprolite, which is the substratum of the former giant Spodosol and probably the last material preserved upon the bedrock.

5.4. *The sequences of evolution*

Based on these soil transformations, two main evolutionary sequences can be proposed with regard to landform evolution: (1) the hilly landform sequence: convex hills–low hills–hills with flat interzones; (2) the plain landform sequence: ferrallitic plains–podzolic plains–peat soils–flood depressions.

The origin of the initial landform of each evolutionary sequence remains unknown, since it has not been studied. Nevertheless, the multi-convex landform is probably

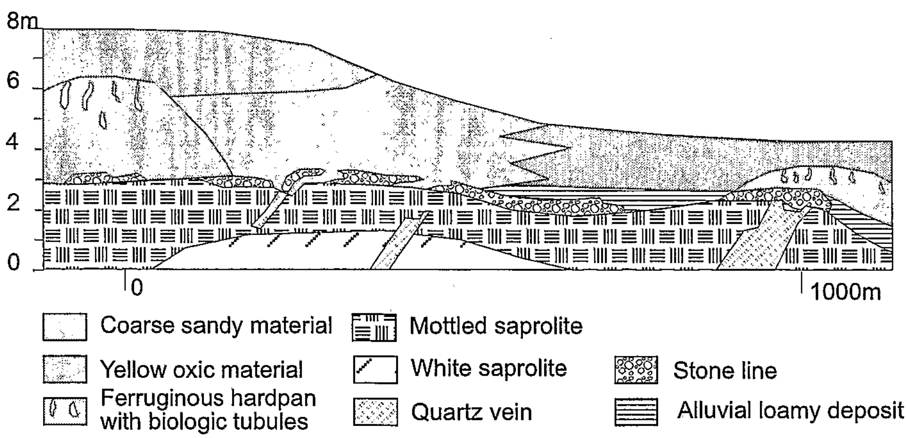

Fig. 13. A natural cut along the Ocamo river bank exhibits a yellow sediment deposited upon an evenly eroded weathering profile with intercalated ironcrusts. They are pedorelicts from ancient contrasted seasonal climatic conditions. In this region, an intense denudation followed by a broad sediment deposit could have originated the ferrallitic plain covered with yellow Oxisols.

genetically connected with former higher planation surfaces and particularly with the Upper multi-convex surface, its direct neighbour at higher altitudes (Gavaud et al., 1986). The lack of geomorphic continuity between these two surfaces, usually separated by an escarpment 50 to 150 m high, does not allow the observation of a continuous gradation, except in some parts of the Orinoco basin (Atlas del Inventario de Tierras del Territorio Federal Amazonas, 1987) where a rolling landform 5 to 10 km wide joins the two surfaces. Elsewhere, any continuous gradation is interrupted by escarpments corresponding with the margins of large granite batholiths.

The origin of the ferralitic plain, with its continuous mantle of yellow Oxisols, still lingers in the shadows. Is it the result of a pedogenic episode or an erosion episode? A continuous transition is observed between the rolling landforms and the flat ferrallitic landforms, but these two mantles frequently present very different soils. One has Oxisols and Ultisols with oxide nodules and concretions, while the other has yellow Oxisols without nodules. This lack of continuity may also have a geological origin, as observed in the northern part of the basin. A natural cut in the Ocamo river bank (Fig. 13), which crosses an extensive ferrallitic plain, shows a yellow sediment deposited upon an evenly eroded weathering profile with intercalated ferricretes. These are probably remnants of ancient soils formed under contrasted climatic conditions. Here, undoubtedly, an erosion episode followed by a huge sediment deposit built the ferrallitic plain after a long period during which conditions for widespread denudation and sediment transport prevailed.

6. Conclusion

It is normally admitted that, under humid tropical climate, soils with Spodosol-like profiles develop only from sandy materials related to geological deposits and intrinsically poor in clay minerals. Sequence studies in the Rio Negro Basin, where Spodosols are closely contiguous with other clayey soils, show that Spodosols may also develop in clay-poor materials formed in situ without any transport. Spodosols may thus be considered as a link in soil catenas. These observations, in addition to others from different Amazon regions, convey the idea that Spodosol formation is a process involving lateral soil transformation, of broad occurrence in the Amazon basin, at least in its most humid regions. This concept is in accordance with the theory of evolution and dynamics of the soil mantle as geomorphic processes (Millot, 1983).

The soil transformations highlighted by the catena studies are: (i) the gradual clay eluviation and oxide removal from the hilly landscape, (ii) the destruction of the Oxisol mantle and the formation of albic and spodic horizons, and (iii) the destruction of the sandy mantle in the plains. These processes are thought to exert a direct influence on the landform evolution. The multi-convex landform with Oxisols and Ultisols can be gradually transformed into a smooth undulating landform with Ultisols and Spodosols. The ferrallitic plain with Oxisols can be gradually transformed into a flat surface with hydromorphic Spodosols. The sandy mantle generated by the podzolisation can be, in certain conditions, transformed into Histosols. This evolution is actually achieved in the lower areas of the Rio Negro basin, where the sandy mantle is completely eroded, and where only a thin organic blanket persists on the remaining white saprolite. Under these conditions, the final stable pedologic cover appears to be the white saprolite, otherwise referred to as kaolinitic pallid zone.

Obviously, more studies are needed to grasp the exact origin of the ferrallitic plain and the causes of soil diversification in the hilly landscape.

Acknowledgements

This work has been carried out within the frame of the CNPq (Brazil)-ORSTOM (France) agreement. We are very grateful to the support provided by Professor Adolfo J. Melfi (Geosciences Institute of Sao Paulo University), Professor Carlos C. Cerri (CENA, Sao Paulo University) and to the helpful collaboration of Helcio Andrade (Lavras University), Angelo A. Dos Santos and Donato Nobre (INPA Manaus) during the field trips.

Appendix A. Soil profile descriptions

Depth (cm)	Horizon name	Color (moist)	Texture	Structure	Coarse elements
Sequence 1: Profile F1. Rhodic Kandiudult					
0–30	Brown humic	Dark brown (10YR4/3)	Sandy loam (20%)	Fine blocky to crumb	
30–60	Pale humic	Yellowish brown (10YR5/4)	Sandy clay (50%)	Fine rounded grain	
60–80	Yellow oxic	Yellow (7.5YR5/8)	Sandy clay (50%)	Fine blocky	
80–150	Red oxic	Red brown (2.5YR3/6)	Clayey (60%)	Medium blocky	
150–180	Mottled saprolite	Yellowish brown (10YR5/6), red (10R3/6) mottles	Silty clay (50%)	Medium to coarse blocky	
180–300	Red saprolite	Red brown (2.5YR3/6), dark red (10R3/4) mottles	Silty clay (45%)	Medium blocky	Micaceous soft nodules with parent rock fabric
Sequence 1: Profile F2. Typic Kandiudult					
0–35	Brown humic	Dark yellowish brown (10YR4/3) Dark brown (10YR4/3)	Sandy loam (20%)	Medium crumb to subangular blocky	
35–55	Pale humic	Yellowish brown (10YR5/4)	Sandy clay loam (30%)	Fine round grain	
55–130	Pale humic	Yellowish brown (10YR6/4)	Sandy clay (40%)	Medium blocky	
130–220	Yellow oxic	Yellow (10YR6/6)	Sandy clay-clayey (45%), fine sand	Fine blocky	
220–280	Pseudo-gley	Pale yellow (5Y7/3), irregular yellow (10YR5/6) mottles	Sandy clay (40%)	Massive	
Sequence 2: Profile F3. Gibbsitic Clayey-squeletal Hapludox					
0–10	Brown humic	Brown (10YR 5/6)	Sandy clay loam (30%)	Medium subangular blocky and fine rounded grain	
40–80	Yellow oxic	Yellow (7.5YR 5/6)	Clayey	Fine round grain	
80–180	Yellow oxic	Yellow (7.5YR 5/6)	Clayey	Fine rounded grain	Very abundant dark red (10R 3/4) gibbsitic concretions and indurated blocks
180–310	Red oxic	Red (2.5YR 5/8)	Clayey to clay–loam (60%)	Fine grain	Very abundant concretions and indurated blocs

310–440	Red saprolite	Red (2.5YR 4/8), dark red (10R 3/4) compact mottles	Clayey fine material (60%)	Fine blocky	Darkred fragments of weathered rock
Sequence 2: Profile F6. Typic Hapludox					
0–20	Brown humic	Pale brown (10YR 4/4)	Sandy clay loam (30%)	Subangular blocky to crumb	
20–80	Yellow oxic	Yellow (7.5YR 5/6)	Clayey	Fine blocky	
80–120	Red oxic	Red (5YR 5/8)	Clayey	Granular	
120–280	Red oxic	Pale red (2.5YR 4/8)	Clayey	Fine grain	Abundant concretions with dark red (10R 3/4) core
280–300	Plinthite	Pale red (2.5YR 4/8)	Clayey	Fine blocky	
300–390	Red saprolite	Pale red (2.5YR 5/8), many prominent dark red (10R 4/8) mottles with micas	Loamy clay	Fine angular blocky	
390–400	Mottled saprolite	Pale red (2.5YR 5/8), large pale (10YR 8/6) mottles	Loamy clay	Fine angular blocky	
Sequence 2: Profile F4. Plinthic Kandiaquult					
0–30	Brown humic	Pale brown (10YR 3/4)	Sandy fine sand	Medium crumb	
30–60	Pale humic	Pale yellow (10YR 5/4)	Sandy loam (15%), fine and medium sand	Rounded granular	
60–70	Albic	Yellowish brown (10YR 4/4)	Sandy, medium sand	Massive	
70–100	Plinthite	Grey (2.5Y 7/4) wet, many diffuse rounded brownish-yellow (10YR 6/8) mottles	Sandy loam (20%)	Medium subangular blocky	Quartzitic coarse sand and quartz gravel line at the bottom
100–140	Mottled saprolite	Grey (2.5Y 7/2), irregular diffuse yellowish-brown (10YR 6/6) mottles	Sandy clay loam (30%), coarse sand	Fine angular blocky, water-saturated	
140–150	White saprolite	Pale grey (5Y 7/1), yellow (10YR 6/6) mottles around roots and channels	Clayey (50%)	Water-saturated	

Appendix A. Soil profile descriptions

Depth (cm)	Horizon name	Color (moist)	Texture	Structure	Coarse elements
Sequence 3: Profile F1, Plinthic Kandiudox					
0–10	Brown humic	Brown (10YR 3/3)	Silt-loam, fine sand	Crumb	
10–50	Pale humic	Brownish yellow (10YR 4/4)	Sandy loam (15%), fine and medium sand	Prominent medium crumb and fine rounded grain	
50–100	Yellow oxic	Yellow (10YR 5/6)	Sandy clay (40%), medium sand	Prominent fine angular blocky	Many indurate blocks
100–120	Red oxic	Red-brown (7.5YR 5/6)	Clayey (60%), fine sand	Medium blocky and fine rounded grain	Quartz gravel and indurate blocks
120–170	Plinthite	Strong brown (7.5YR 5/8), many red (5YR 5/6) mottles	Clayey (60%), fine sand	Moderate coarse blocky	
170–240	Mottled saprolite	Pale red (2.5YR 4/8), many large irregular (10YR 7/4) mottles	Clayey (60%)	Massive	
Sequence 3: Profile F2. Arenic Umbric Kandiaquult					
0–10	Brown humic	Dark reddish brown (5YR 3/2)	Silt loam	Fine crumb structure	Abundant fine and medium roots
10–30	Albic	Pale ochre (10YR 5/3)	Sandy, coarse sand	Single grain structure	
30–60	Black humic	Dark brown (10YR 3/3) wet	Sandy, medium sand	Massive	
60–100	Eluviated	Yellow (10YR 5/6)	Sandy loam, medium sand (15%)	Massive	
100–180	Pseudo-gley	Yellowish brown (10YR 5/6)	Sandy clay loam (30%)	Massive	
180–250	White saprolite	Yellowish grey (2.5Y 7/2)	Sandy clay (40%)	Massive, water-saturated	
250–360	Regolith	Light grey (2.5Y 7/4), large reddish yellow (7.5YR 6/6) mottles	Sandy clay loam (20%), coarse quartz	Massive, water-saturated	Few weathered feldspars and micas
Sequence 3: Profile F3. Ultic Tropaquod					
0–10	Black humic	Dark brown (5YR 3/2)	Silty loam (30% OM)	Fine crumb	Leaves and plant fragments

10–30	Black humic	Dark brown (10YR 4/2)	Sandy	Massive and weak medium crumb	
30–60	Albic	White (10YR 7/2)	Sandy, medium sand	Massive	
60–65	Spodic	Dark greyish brown (10YR 3/6)	Sandy, medium sand	Massive	
65–90	Albic	White (10YR 7/2)	Sandy, medium sand	Massive, water-saturated	
90–105	Spodic	Dark grey (10YR 3/2)	Sandy	Massive, water-saturated	
65–90	Albic	White (10YR 7/2)	Sandy, medium sand	Massive, water-saturated	
90–105	Spodic	Dark grey (10YR 3/2)	Sandy	Massive, water-saturated	
105–110	Alios	Dark brown (7.5YR 3/4)	Loamy sand, coarse sand	Laminar	
110–150	White saprolite	Pale grey (5Y 7/2)	Sandy clay (4%), coarse sand	Massive, water-saturated	
Sequence 4: Profile S5. Xanthic Acrudox					
0–20	Brown humic	Brown (10YR 5/3) wet	Sandy clay loam, (30%) fine sand	Clear medium crumb	
20–60	Pale humic	Yellowish brown (10YR 5/4)	Sandy Clay (40%)	Very fine granular	
60–180	Yellow oxic	Reddish yellow (7.5YR 6/6)	Clayey (60%)	Very fine angular blocky	
180–220	Plinthite	Yellow (10YR 6/4), common medium rounded red (5YR 5/6) mottles	Clayey	Massive and coarse blocky	
220–250	Mottled saprolite	Pale grey (2.5Y 7/2), coarse irregular, prominent red (5YR 5/8) mottles	Clay loam (50%)	Massive	
Sequence 4: Profile F2. Plinthic Kandiudult					
0–10	Brown humic	Brown (10YR 5/3)	Sandy clay (40%), fine sand	Medium crumb	Roots
10–40	Pale humic	Light brownish grey (2.5Y 6/2)	Clay (40%)	Moderate very fine granular, rounded	
40–110	Yellow oxic	Yellow (10YR 6/4)	Clayey (60%)	Massive and very fine angular blocky	
110–210	Plinthite	Light grey (2.5Y 7/2), common medium rounded mottles with a red center (2.5Y 4/8) and ochre (7.5YR 5/8) border	Clayey (60%)	Massive and moderate coarse blocky	

Appendix A. Soil profile descriptions

Depth (cm)	Horizon name	Color (moist)	Texture	Structure	Coarse elements
210–330	Mottled saprolite	Pale grey (5Y 8/2)	Clayey (70%), medium sand	Massive, water-saturated	
330–350	White saprolite	Grey (2.5Y 8/4), many coarse yellow (10YR 7/6) mottles	Sandy clay loam (30%), coarse sand	Massive, water-saturated	Kaolinized feldspars
Sequence 4: Profile S4, Albic Paleaquult					
0–10	Fibrous humic	Dark brown (7.5YR 4/2)	Sandy loam, coarse sand	Medium crumb	Abundant fine roots
10–40	Black humic	Dark brown (7.5YR 4/2)	Sandy (< 10%)	Weak, medium crumb	
40–130	Albic	Light brownish grey (2.5Y 5/4)	Sandy	Massive, water-saturated	
130–175	Compact albic	Yellowish brown (10YR 5/4)	Sandy (< 10%)	Massive, water-saturated	
175–220	White saprolite	Light grey (5Y 6/2)	Sandy clay (30%)	Massive, water-saturated	Without visible coarse quartz
Sequence 4: Profile F5. Arenic Grossarenic Tropaquod					
0–3	Fibrous humic	Red brown (7.5YR 3/3)	Loamy, Organic	Organic crumb	Mat of fine roots
3–20	Black humic	Brown (10YR 5/3)	Sandy	Weak, medium crumb	
20–180	Albic	White (10YR 7/2)	Sandy	Single grain, water-saturated	
180–200	Spodic, alios	Dark brown (10YR 3/6), black superficial organic coating	Sandy to silt loam	Compact with horizontal foliated substructure	
Sequence 5: Profile F1. Hydric Tropofibrist					
0–5	Litter				Leaves and plant fragments
5–25	Fibrous humic	Red brown (5YR 3/2)	Organic (60% OM)	Weak, medium crumb	Mat of fine and medium roots
25–45	Black humic	Dark brown (7.5YR 3/2)	Organic (30% OM), fine sand	Medium crumb	Roots

45–60	Albic	White (5Y 8/2)	Sandy, coarse sand	Single grain, water-saturated	
60–65	Spodic	Dark brown (10YR 3/6)	Sandy loam (10%)	Massive, water-saturated	
65–80	Argillic	Yellowish brown (10YR 4/3)	Sandy loam (10%)	Massive, water-saturated	
Sequence 5: Profile F2. Histic Tropaquod					
0–10	Fibrous humic	Dark brown (10YR 4/2)	Organic (50% OM)	Some crumb aggregates	Mat of fine roots
10–40	Black humic	Dark brown (10YR 4/2)	Sandy loam (20% OM)	Single grain	
40–105	Albic	White (2.5Y 7/2)	Sandy, medium sand	Single grain	
105–120	Compact albic	White (2.5Y 7/2)	Sandy, medium sand	Massive, water-saturated	
120–123	Spodic	Dark brown (10YR 3/6)	Sandy loam, fine sand	Massive, water-saturated	
123–160	Argillic	Greyish brown (10YR 6/4)	Sandy loam, fine sand	Massive, water-saturated	
160–200	Albic	White (2.5Y 7/2)	Sandy, coarse and medium sand	Single grain, water-saturated	
Sequence 5: Profile S3. Typic Quartzipsamment					
0–5	Litter				Leaves and plant residues
5–25	Fibrous humic	Dark brown (5YR 5/2)	Sandy loam, fine sand (20% OM)	Fine crumb	Fine roots
25–65	Black humic	Dark brown (10YR 3/3)	Sandy, medium sand	Massive	
65–200	Albic	Pale grey (10YR 7/1)	Sandy, medium and fine sand	Single grain	
200–420	Albic	White (5Y8/1)	Sandy loam, medium and coarse sand	Massive	
Sequence 6: Profile F1. Aeric Grossarenic Tropaquod					
0–5	Fibrous humic				Leaves and fine roots
5–20	Black humic	Brown (10YR 5/3)	Sandy	Single grain	
20–170	Albic	White (10YR 7/2)	Sandy	Single grain	
170–180	Spodic	Dark grey (10YR 3/2)	Sandy	Massive, water-saturated	
180–185	Alios	Dark brown (7.5YR 3/4)	Loamy sand, coarse sand	Laminar, water-saturated	
185–220	White saprolite	Pale grey (5Y 7/2), Pale yellow (10YR 7/6) mottles along channel voids	Sandy clay, coarse sand (40%)	Massive, water-saturated	

Appendix A. Soil profile descriptions

Depth (cm)	Horizon name	Color (moist)	Texture	Structure	Coarse elements
Sequence 6: Profile F2. Histic Tropaquod					
0–30	Fibrous humic	Dark brown (7.5YR 4/2)	Organic (30% OM)	Crumb aggregates	Dead leaves and plant fragments
30–50	Black humic	Dark brown (10YR 3/3)	Sandy	Very weak medium subangular	
50–80	Albic	White (10YR 7/2)	Sandy	Single grain	
80–120	Argillic	Light brownish grey (2.5Y 6/2)	Sandy	Weak medium blocky	
120–160	Albic	White (10YR 7/2)	Loamy sand, coarse sand	Massive	
160–165	Spodic	Dark grey (10YR 3/2)	Sandy	Massive, water-saturated	
165–210	White saprolite	Pale grey (5Y 7/2)	Sandy clay loam (30%), coarse sand	Massive, water-saturated	
Sequence 6: Profile F3. Arenic Kandiaquult					
0–10	Fibrous humic	Dark brown (7.5YR 4/2)	Organic (30% OM)	Weak crumb	Dead leaves and fine roots
10–20	Black humic	Dark brown (10 YR 3/3)	Sandy loam, fine sand	Very weak medium subangular	
20–50	Albic	Light grey (2.5Y 7/2)	Sandy (7%)	Single grain	
50–105	Argillic	Light brownish grey (2.5Y 6/2), elongated dark organic (10YR 4/3) mottles along root channels	Sandy loam (17%)	Weak medium blocky	
105–180	White saprolite	Light grey (5Y 7/2)	Sandy clay loam (30%), coarse sand	Massive, water-saturated	
Sequence 6: Profile S1. Typic Albaquult					
0–5	Fibrous humic	Dark brown (7.5YR 4/2)			Dead leaves and fine roots
5–15	Black humic	Dark brown (10YR 4/3)	Sandy with fine sand		
15–30	Albic	White (10YR 7/2)	Sandy	Single grain	
30–50	White saprolite	Light olive grey (5Y 6/2), pale yellow (2.5Y 7/6) mottles along voids and channels	Sandy clay loam (30%), coarse sand	Massive, water-saturated	
50–180	White saprolite	Light grey (5Y 7/2)	Sandy loam (20%), coarse sand	Massive, water-saturated	

Appendix B. Glossary

Albic	White quartz sand-sized grains without any clay (includes a compact type with silt-sized grains)
Alios	Brown or greyish sometimes weakly organic silico-aluminous pan or Bs horizon
Argillic	Kaolinite or vermiculite clay-rich layer with visible clay coatings
Black humic	With black illuvial organic matter not bound to minerals
Brown humic	Acid with organic matter bound to clay minerals
Concretions	Indurated irregular oxide-rich gravel with a polished cortex
Eluvial	Clay-poor or E horizon, almost entirely of sand-sized quartz grains with coatings or microaggregates or bridges of fine material
Fibrous humic	Forest surface tier composed of humic pellets enclosed in a thick root mat
Gley	Permanent water-table, greyish colour with thin, temporary, yellow coloured iron coatings
Indurated blocks	Coarse-indurated fragments of soil material or regolith
Nodules	Rounded oxide-rich gravel-sized element with an undifferentiated fabric
Oxic	Red type or yellow type, soft with 0.05 to 0.1 mm grain structure (microaggregates) or fine blocky structure
Pale humic	Pale yellow or brown, bioturbated with 1% to 2% indiscernible organic matter, soft, 0.5 to 1.5 mm rounded grain structure
Plinthite	Clayey to sandy-clay material with nodular oxide dots in a pale matrix
Pseudogley	Temporary water-table, pale ochre and yellow coloured dots, permanent iron coatings in a sandy-clay material
Regolith	Coarse sandy clay material with primary residual minerals other than quartz and remnants of parent rock fabric
Saprolite	Massive clayey material (includes red, mottled, and white types) with primary residual minerals other than quartz
Spodic	Black illuvial organic compact pan or Bh horizon

References

Aleva, G.J.J., 1981. Bauxitic and other duricrusts on the Guaiana Shield, South America. In: Krishnaswamy, V.S. (Ed.), Lateritisation Processes. Proc. Internat. Sem. on Lateritisation Processes, Trivandum, India, 1979. IBH Publ., New-Delhi, pp. 261–269.

Atlas del Inventario de Tierras del Territorio Federal Amazonas, 1987. Atlas géomorfopedológico. Escala 1/250000. ORSTOM and Ministerio del Ambiente y de los Recursos Naturales Renovables, Dirección de Suelos, Vegetación y Fauna, Caracas, Venezuela.

Berthelin, J., Munier-Lamy, C., Wedraogo, F.X., Belgy, G., Bonne, M., 1990. Mécanismes microbiens d'acidification et d'altération intervenant dans les sols bruns et dans les podzols forestiers. Synthèse et discussion de travaux antérieurs. Sci. du Sol 28 (4), 301–318.

Boulet, R., Brugière, J.M., Humbel, F.X., 1979. Relation entre organisation des sols et dynamique de l'eau en Guyane Française septentrionale. Conséquences agronomiques d'une évolution dominée par un déséquilibre d'origine principalement tectonique. Sci. du Sol 1, 3–18.

Boulet, R., Chauvel, A., Humbel, F.X., Lucas, Y., 1982. Analyse structurale et cartographie en Pédologie. 1—Prise en compte de l'organisation bidimentionnelle de la couverture pédologique: les études de toposéquences et leurs principaux apports à la connaissance des sols. Cah. ORSTOM sér. Pédol. 19 (4), 309–321.

Boulet, R., Chauvel, A., Lucas, Y., 1984. Les systèmes de transformation en pédologie. AFES, Livre Jubilaire du Cinquantenaire. Plaisir, France, pp. 167–179.

Blancaneaux, Ph., 1985. Organisation et comportement hydrologique de deux couvertures pédologiques sur granito-gneiss, région de Grégoire, Guyane Fr. Thèse, Univ. d'Orléans, France, 274 pp.

Blakemore, L.C., 1983. Acid oxalate-extractable iron, aluminium and silicon. ICOMAND Circular Letter No. 5, New Zealand Soil Bureau, Appendix 1.

Bravard, S., Righi, D., 1990. Podzols in Amazonia. Catena 17, 461–475.

Bullock, P., Jongerius, A., Fedoroff, N., Stoops, G., Tursina, T., 1985. In: Waine Research (Ed.), Handbook for Soil Thin Section Description. Albrighton WV, England, 150 pp.

Cecilia Martin, F., 1976. Atlas Géologique du Monde, feuilles 4 et 5: Amérique du Sud. 1/1000000. UNESCO Paris.

Chauvel, A., Lucas, Y., Boulet, R., 1987. On the genesis of the soil mantle of the region of Manaus, Central Amazonia, Brazil. Experientia 43, 234–241.

Choubert, B., 1974. Le Précambrien des Guyanes. Mém. BRGM no. 81, Paris, 204 pp.

Cornu, S., Lucas, Y., Desjardins, T., Nitshe, S., 1995. Rapidité de la vitesse d'altération des minéraux du sol en conditions ferrallitiques. Méthodes des minéraux-test. C.R. Acad. Sci., Sér. IIa Paris 317, 311–316.

Dubroeucq, D., Blancaneaux, Ph., 1987. Les podzols du haut rio Negro, région de Maroa, Vénézuéla. Environnement et relations lithologiques. In: Righi, D., Chauvel, A. (Ed.), Podzols et Podzolisation, AFES (Plaisir)-INRA (Paris), pp. 37–52.

Dubroeucq, D., Sanchez, V., 1981. Caracteristicas edaficas y ambientales del area muestra San Carlos de rio Negro—Solano. Serie Informe Técnico, DGSIIA/IC/12, MARNR, Caracas, Vénézuéla.

Dubroeucq, D., Volkoff, B., 1988. Evolution des couvertures pédologiques sableuses à podzols géants d'Amazonie, bassin du haut rio Negro. Cah. ORSTOM sér. Pédol. 24 (3), 191–214.

Dubroeucq, D., Gavaud, M., Millot, G., 1988. A high bauxitic surface in the Amazon Territory of Venezuela. Mapping through the Radar-Slar imagery and exploratory examination. Sci. Géol. Bull. 41 (1), 99–111, Strasbourg, France.

Dubroeucq, D., Volkoff, B., Pedro, G., 1991. La couverture pédologique du Bouclier Nord de l'Amazonie (bassin du Haut Rio Negro)—Séquence évolutive des sols et son rôle dans l'aplanissement généralisé des zones tropicales perhumides. C.R. Acad. Sci., sér. II Paris 312, 663–671.

Eyrolle, F., 1994. La fraction colloïdale organique dans les processus de transport des métaux dans les eaux de surface: application aux systèmes d'altération en milieu tropial (Brésil). Thèse, Univ. Aix-Marseille III, France, 334 pp.

Eyrolle, F., Fevrier, D., Benaim, J.Y., 1993. Etude par DPASV de l'aptitude de la matière organique colloïdale à fixer et à transporter des métaux. Exemple de bassins versants en zone tropicale. Environ. Technol. 14, 701–717.

Fritsch, E., 1984. Les transformations d'une couverture ferrallitique en Guyane Française. Thèse, Univ. Paris VII, ORSTOM-Paris.

Fritsch, E., Peterschmitt, E., Herbillon, A.J., 1992. A structural approach of the regolith: identification of structures, analysis of structural relationships and interpretations. Sci. Géol. Bull. 45 (2), 77–97.

Fritsch, J.M., 1992. Les effets du défrichement de la forêt amazonienne et de la mise en culture sur l'hydrologie de petits bassins versants. Opération ECEREX en Guyane Française. ORSTOM-Paris, 392 pp.

Fritsch, E., Bocquier, G., Boulet, R., Dosso, M., Humbel, F.X., 1986. Les systèmes transformants d'une couverture ferrallitique de Guyane Française. Analyse structurale d'une formation supergène et mode de représentattion. Cah. ORSTOM sér. Pédol. 22 (4), 361–396.

Gavaud, M., Blancaneaux, Ph., Dubroeucq, D., Pouyllau, M., 1986. Les Paysages pédologiques de l'Amazonie vénézuélienne. Cah. ORSTOM sér. Pédol. 22 (3), 265–284.

Grimaldi, C., Pédro, G., 1996. Importance de l'hydrolyse acide dans les systèmes pédologiques des régions tropicales humides. C.R. Acad. Sci., Sér. IIa Paris 323, 483–492.

Grimaldi, C., Fritsch, E., Boulet, R., 1994. Composition chimique des eaux de nappe et évolution d'un matériau ferrallitique en présence du système muscovite–kaolinite–quartz. C.R. Acad. Sci., Sér. II Paris 319, 1383–1389.

Harrassowitz, H., 1926. Laterit. Forsch. Geol. Paleont. 4, 253–565, Berlin.

Hétier, J.M., Jeanroy, E., 1973. Solubilisation différentielle du fer, de la silice et de l'aluminium par le réactif oxalate–dithionite et la soude diluée. Pédologie 23 (2), 85–99.

Hole, F.D., 1961. A classification of pedoturbations and some other processes and factors of soil formation in relation to isotropism and anisotropism. Soil Sci. 91, 375–377.

Jeanroy, E., 1983. Diagnostique des formes du fer dans les pédogénèses tempérées. Evaluation par les rèactifs chimiques d'extraction et apports de la spectrométrie Mossbauer. Thèse Doc. Univ. Nancy I, France, 157 pp.

Johnson, D.L., 1985. Soil thickness processes. In: Jungerius, P.D. (Ed.), Soils and Geomorphology. Catena Suppl. 6, pp. 29–57. Braunschweig, Germany.

Klinge, H., 1965. Podzol soils in the Amazonian basin. J. Soil Sci. 16, 96–103.

Lips, J.M., Duivenvoorden, J.F., 1994. Geomorphic and lithostratigraphic evidence of Pleistocene climatic change in Amazonia: new data from the middle Caqueta area, Colombia. Geo-Eco-Trop 16, 21–47.

Liu, K., Colinvaux, P.A., 1985. Forest changes in the Amazon basin during the last glacial maximum. Nature 318, 556–557.

Lucas, Y., 1989. Systèmes pédologiques en Amazonie brésilienne. Equilibres, déséquilibres et transformations. Thèse Univ. Poitiers, Géochimie de la Surface, 153 pp.

Lucas, Y., Boulet, R., Chauvel, A., Veillon, L., 1987. Systèmes sols ferrallitiques—Podzols en région amazonienne. In: Righi, D., Chauvel, A. (Ed.), Podzols et Podsolisation. AFES, Plaisir—INRA, Grignon, pp. 53–65.

Lucas, Y., Luizäo, F.J., Chauvel, A., Rouiller, J., Nahon, D., 1993. The relation between biological activity of the rain forest and mineral composition of the soils. Science 260, 521–523.

Lucas, Y., Nahon, D., Cornu, S., Eyrolle, F., 1996. Genèse et fonctionnement des sols en milieu équatorial. C.R. Acad. Sci., Sér. IIa Paris 322, 1–16.

Mehra, O.P., Jackson, M.L., 1960. Iron oxide removal from soils and clays by a dithionite-citrate system buffered with sodium bicarbonate. Clays Clay Miner. 7, 317–327.

Millot, G., 1983. Planation of continents by intertropical weathering and pedogenetic processes. In: Melfi, A.J., Carvalho, A. (Ed.), Lateritisation Processes. Univ. of Sao Paulo Press, Sao Paulo, pp. 53–63.

Mendoza, V., Moreno, L., Barrios, F., Rivas, D., 1977. Geología de la parte Norte del Territorio Federal Amazonas, Venezuela. 5e Cong. Geol. Venezolano. Ministerio de Energía y Minas—Sociedad Venezolana de Geólogos ed., Memoria I, pp. 363–406.

Norrish, K., Taylor, R.M., 1962. Quantitative analysis by X-ray diffraction. Clay Miner. Bull. 5, 98–109.

Pédro, G., 1966. Intérêt géochimique et signification minéralogique du paramètre moléculaire Ki = SiO_2/Al_2O_3 dans l'étude des latérites et des bauxites. Bull. Gr. Fr. Argiles 18, N.S. 13, 19–31.

Pimentel da Silva, L., Hodnett, M.G., Rocha, H.R., Cruz Senna, R., 1992. A comparison of dry season soil water depletion beneath central amazonian pasture and rain forest. 7 Congresso Brasileiro de Meteorología. Anaís vol. 1. Sociedade Brasileira de Meteorología, Sao Paulo SP, pp. 308–313.

Projeto Radambrasil, 1976. Levantamento de Recursos Naturais, folha NA-19, Vol. 11: Pico da Neblina. Ministerio das Minas e Energia, Departamento Nacional da Produçâo Mineral, Rio de Janeiro, 374 pp.

Putzer, H., 1984. The geological evolution of the Amazon basin and its mineral resources. In: Sioli, H. (Ed.), The Amazon, Limnology and Landscape Ecology of a Mighty tropical river and its basin. Dr W. Junk Publishers, Dordrecht, The Netherlands, pp. 15–46.

Roche, M.A., 1981. Watershed investigations for development of forest resources of the Amazonian region in French Guyana. In: Lal, R., Russel, E.W. (Eds.), Tropical Agricultural Hydrology, Wiley, Chichester, UK, pp. 75–92.

Schnütgen, A., Bremer, H., 1985. Die Entstehung von Decksanden im oberen Rio Nego-Gebiet. Z. Geomorph. N.F., Suppl.-Bd. 56, 55–67.

Servant, M., Fontes, J.-C., Rieu, M., Saliège, J.-F., 1981. Phases climatiques arides holocènes dans le sud-ouest de l'Amazonie (Bolivie). C.R. Acad. Sci., Sér. II Paris 292, 1295–1297.

Soil Survey Staff, 1975. Soil taxonomy. Basic system of soil classification for making and interpreting soil surveys. USDA, Washington, Agric. Handbook 436, 754 pp.
Soil Survey Staff, 1990. Keys to Soil Taxonomy. Agency for International Development. USDA Soil Management Support Services. Technical monograph 19, 4th edn. Virginia Polytechnic Institute and State University.
Sombroek, W.G., 1966. Amazon Soils. A reconnaissance of the soils of the Brazilian Amazon region. PUDOC, Wageningen, The Netherlands, 300 pp.
Sombroek, W.G., 1990. Amazon landforms and soils in relation to biological diversity. In: Annual Report 1990. International Soil Reference and Information Center, Wageningen, The Netherlands, pp. 7–25.
Thomas, M.F., 1994. Case-studies of Podzolisation from Amazonia and Guyana, pp. 45-47. In: Geomorphology in the Tropics, Wiley, Chichester, UK, 433 pp.
Thornber, M.R., 1992. The chemical mobility and transport of elements in the weathering environment. In: Butt, C.R.M., Zeegers, H. (Ed.), Handbook of Exploration Geochemistry, Vol. 4. Regolith Exploration Geochemistry in Tropical and Subtropical Terrains. Elsevier, 607 pp.
Tricard, J., 1974. Existence de périodes sèches au Quaternaire en Amazonie et dans les régions voisines. Rev. Géomorphol. Dyn. 23, 145–158.
Turenne, J.F., 1975. Modes d'humification et différenciation podzolique dans deux toposéquences guyanaises. Thèse Univ. Nancy. Mém. ORSTOM no. 84, Paris, 173 pp.
Veillon, L., 1990. Sols ferrallitiques et podzols en Guyane septentrionale. Relations entre systèmes de transformations pédologiques et évolution historique d'un milieu tropical humide et forestier. Thèse Univ. Paris 6, France, 191 pp.
Volkoff, B., Mortatti, J., Cerri, C.C., 1990. Rôle des nappes dans les différenciations pédologiques à podzols de l'Amazonie. C.R. Acad. Sci., Sér. II Paris 310, 1361–1368.

(Continued from inside front cover)

Orders, claims, and product enquiries: please contact the Customer Support Department at the Regional Sales Office nearest you:
New York, Elsevier Science, P.O. Box 945, New York, NY 10159-0945, USA. Tel: (+1) 212-633-3730, [Toll free number for North American customers: 1-888-4ES-INFO (437-4636)], Fax: (+1) 212-633-3680, E-mail: usinfo-f@elsevier.com
Amsterdam, Elsevier Science, P.O. Box 211, 1000 AE Amsterdam, The Netherlands. Tel: (+31) 20-485-3757, Fax: (+31) 20-485-3432, E-mail: nlinfo-f@elsevier.nl
Tokyo, Elsevier Science, 9-15, Higashi-Azabu 1-chome, Minato-ku, Tokyo 106, Japan. Tel: (+81) 3-5561-5033, Fax: (+81) 3-5561-5047, E-mail: info@elsevier.co.jp
Singapore, Elsevier Science, No. 1 Temasek Avenue, #17-01 Millenia Tower, Singapore 039192. Tel: (+65) 434-3727, Fax: (+65) 337-2230, E-mail: asiainfo@elsevier.com.sg

US mailing info – *Catena* (ISSN 0341-8162) is published bimonthly by Elsevier Science B.V. (Molenwerf 1, P.O. Box 211, 1000 AE Amsterdam). Annual subscription price in the USA US$ 810.00 (valid in North, Central and South America), including air speed delivery. Periodicals postage paid at Jamaica, NY 11431.
USA POSTMASTERS: Send address changes to Catena, Elsevier Science Regional Sales Office, Customer Support Department, 655 Avenue of the Americas, New York, NY 10010-5107, USA. AIRFREIGHT AND MAILING in the USA by Elsevier Science Regional Sales Office, Customer Support Department, 655 Avenue of the Americas, New York, NY 10010-5107, USA.

NOTE TO CONTRIBUTORS

Guide to Authors
A detailed Guide for Authors is available upon request. The guide can also be found on the World Wide Web: access under http://www.elsevier.nl or http://www.elsevier.com. Please pay attention to the following notes:

Language
Manuscript should be written in English. Authors whose native language is not English are recommended to seek the advice of a colleague who has English as his mother-tongue before submitting their manuscript.
Authors in Japan please note: Upon request, Elsevier Science Japan will provide authors with a list of people who can check and improve the English of their paper (*before submission*). Please contact our Tokyo office: Elsevier Science Japan, 1-9-15 Higashi Azabu, Minato-ku, Tokyo 106; Tel. +81 5 5561 5032; Fax +81 5 5561 5045.

Preparation of the text
(a) The manuscript should preferably be prepared on a word processor and printed with double spacing and wide margins and include an abstract of not more than 500 words. (b) Authors should use IUGS terminology. The use of S.I. units is also recommended. (c) The title page should include the name(s) of the author(s) and their affiliations, fax and e-mail numbers. In case of more than one author, please indicate to whom the correspondence should be addressed.

Keywords
Except for the journals *Coastal Engineering* and *Hydrometallurgy,* authors should provide 4 to 6 keywords. These must be taken from the most recent Americal Geological Institute GeoRef Thesaurus and should be placed beneath the abstract. Hydrometallurgy authors will be provided with a list of keywords by the editor upon submission of manuscripts.

References
(a) References in the text consist of the surname of the author(s), followed by the year of publication in parentheses. All references cited in the text should be given in the reference list and vice versa.
(b) The reference list should be in alphabetical order.

Tables
Tables should be compiled on separate sheets and should be numbered according to their sequence in the text. Tables can also be sent as glossy prints to avoid errors in typesetting.

Illustrations
(a) All illustrations should be numbered consecutively and referred to in the text.
(b) Colour figures can be accepted providing the reproduction costs are met by the author. Please consult the publisher for further information.

Page proofs
One set of page proofs will be sent to the corresponding author, to be checked for typesetting/editing. The author is not expected to make changes or corrections that constitute departures from the article in its accepted form. Page proofs should be returned within 3 days.

Reprints
Fifty reprints of each article are supplied free of charge. Additional reprints can be ordered on a reprint order form which will be sent to the corresponding author upon receipt of the accepted article by the publisher.

Submission of manuscripts
(a) Manuscripts should be sent in triplicate to the Editorial Office *Catena*, P.O. Box 1930, 1000 BX Amsterdam, The Netherlands.
(b) Illustrations should also be submitted in triplicate. One set should be in a form ready for reproduction: the other two may be of lower quality.
(c) Authors are requested to submit the names, addresses and telephone, facsimile and e-mail numbers of four potential referees with their manuscripts.
(d) The indication of a FAX and e-mail number on the manuscript will assist in speeding communications. The FAX number for the Amsterdam office is: +31-20-4852696.
(e) Submission of an article is understood to imply that the article is original and unpublished and is not being considered for publication elsewhere.

Submission of electronic text
Authors are requested to submit the final text on a 3.5" or 5.25" diskette. It is essential that the name and version of the word processing program, the type of computer on which the text was prepared, and the format of the text files are clearly indicated. Authors are requested to ensure that the contents of the diskette correspond exactly to the contents of the hard copy manuscript. If available, electronic files of the figures should also be included on a separate floppy disk.